

# Early-type Galaxy Distances from the Fundamental Plane and Surface Brightness Fluctuations

John P. Blakeslee,<sup>1,2</sup> John R. Lucey,<sup>2</sup> John L. Tonry,<sup>3</sup> Michael J. Hudson,<sup>4</sup> Vijay K. Narayanan,<sup>5</sup> and Brian J. Barris<sup>3</sup>

<sup>1</sup>Department of Physics and Astronomy, Johns Hopkins University, Baltimore, MD 21218, U.S.A.; *jpb@pha.jhu.edu*

<sup>2</sup>Department of Physics, University of Durham, South Road, Durham, DH1 3LE, United Kingdom; *John.Lucey@durham.ac.uk*

<sup>3</sup>Institute for Astronomy, University of Hawaii, 2680 Woodlawn Drive, Honolulu, HI 96822, U.S.A.; *jt.barris@ifa.hawaii.edu*

<sup>4</sup>Department of Physics, University of Waterloo, ON, N2L 3G1, Canada; *mjhudson@uwaterloo.ca*

<sup>5</sup>Department of Astrophysical Sciences, Princeton University, Princeton, NJ 08544; *vijay@astro.princeton.edu*

Accepted — 2001. Received — ; in original form —

## ABSTRACT

We compare two of the most popular methods for deriving distances to early-type galaxies: the fundamental plane (FP) and surface brightness fluctuations (SBF). Distances for 170 galaxies are compared. A third set of distances is provided by predictions derived from the density field of the *IRAS* redshift survey. Overall there is good agreement between the different distance indicators. We investigate systematic trends in the residuals of the three sets of distance comparisons. First, we find that several nearby, low-luminosity, mainly S0 galaxies have systematically low FP distances. Because these galaxies also have Mg<sub>2</sub> indices among the lowest in the sample, we conclude that they deviate from the FP partly because of recent star formation and consequently low mass-to-light ratios; differences in their internal velocity structures may also play a role. Second, we find some evidence that the ground-based *I*-band SBF survey distances (Tonry et al. 2001) begin to show a bias near the survey limit at  $cz \gtrsim 3500 \text{ km s}^{-1}$ , which is expected for this sort of distance-limited survey, but had not previously been demonstrated. Although SBF and FP distances are affected in opposite senses by errors in the Galactic extinction estimates, we find no evidence for biases in the distances due to Galactic extinction. The tie between the Cepheid-calibrated SBF distances (Mpc) and the far-field calibrated FP distances (km s<sup>-1</sup>) yields a Hubble constant of  $H_0 = 68 \pm 3 \text{ km s}^{-1} \text{ Mpc}^{-1}$ , while the comparison between SBF and the *IRAS*-reconstructed distances yields  $H_0 = 74 \pm 2 \text{ km s}^{-1} \text{ Mpc}^{-1}$  (independent errors only). Thus, there is a marginal inconsistency in the direct and *IRAS*-reconstructed ties to the Hubble flow (this can be seen independently of the SBF distances). Possible explanations include systematic errors in the redshift survey completeness estimates or in the FP aperture corrections, but at this point, the best estimate of  $H_0$  may come from a simple average of the above two estimates. After revising the SBF distances downward by 2.8% to be in agreement with the final set of Key Project Cepheid distances (Freedman et al. 2001), we conclude  $H_0 = 73 \pm 4 \pm 11 \text{ km s}^{-1} \text{ Mpc}^{-1}$  from early-type galaxies, where the second errorbar represents the total systematic uncertainty in the distance zero point. We also discuss the ‘fluctuation star count’  $\bar{N} \equiv \bar{m} - m_{\text{tot}}$ , recently introduced by Tonry et al. (2001) as a less demanding alternative to  $(V-I)$  for calibrating SBF distances. The  $\bar{N}$ -calibrated SBF method is akin to a hybrid SBF-FP distance indicator, and we find that the use of  $\bar{N}$  actually improves the SBF distances. Further study of the behavior of this quantity may provide an important new test for models of elliptical galaxy formation.

**Key words:** galaxies: distances and redshifts — galaxies: elliptical and lenticular, cD — galaxies: fundamental parameters — galaxies: stellar content

## 1 INTRODUCTION

Early attempts to gauge relative distances in samples of elliptical galaxies were based primarily on the colour-magnitude (de Vaucouleurs 1961; Sandage 1972; Sandage & Visvanathan 1978) and Faber-Jackson relations (Faber & Jackson 1976; Schechter 1980; Tonry & Davis 1981), which treated ellipticals as a structurally and chemically homogeneous, single-parameter family. The introduction of the two-parameter fundamental plane (FP), and the closely related  $D_n$ - $\sigma$  relation, by Dressler et al. (1987) and Djorgovski & Davis (1987) allowed for a significant improvement in the measurement of early-type distances. Since then, there has been a proliferation of FP studies, concentrating on the early-type populations within rich clusters (e.g., Lucey & Carter 1988; Lucey et al. 1991a,b,c; Jorgensen et al. 1993, 1996; Prugniel & Simien 1996; Hudson et al. 1997; Pahre et al. 1998; Colless et al. 2001). Although FP measurements have been made at redshifts  $z \approx 0.5$  for galaxy evolution studies (van Dokkum & Franx 1996; Pahre 1998; Kelson et al. 2000b), individual cluster peculiar velocities are only measurable at  $z \lesssim 0.05$ .

The streaming motions of Abell clusters (SMAC) project (Smith et al. 2000, 2001, hereafter SMAC-I and SMAC-II; Hudson et al. 2001, hereafter SMAC-III) is an FP survey with a limiting depth of 12,000 km s<sup>-1</sup>. It combines literature data from  $\sim 20$  different sources with an extensive set of new photometric and spectroscopic observations. A great deal of effort was made in standardizing the data sets to a homogeneous system through intercomparison of data for overlapping galaxies. As a result, the SMAC data set is the largest high-precision FP data set currently available.

In comparison to the FP, the surface brightness fluctuations (SBF) method developed by Tonry & Schneider (1988) has employed a smaller number of researchers. The vast majority of the extant SBF data were collected as part of the ground-based  $I$ -band SBF survey described in detail by Tonry et al. (1997, hereafter SBF-I). This includes the early studies by Tonry, Ajhar, & Luppino (1990) and Tonry (1991), although the results from these early papers have been significantly revised on account of improved analysis methods, better data and standardization of the photometry, new extinction estimates, and a new calibration of the dependence of SBF on the stellar population. The full SBF survey data set, comprising about 300 galaxies within  $cz \lesssim 4000$  km s<sup>-1</sup>, is presented by Tonry et al. (2001, hereafter SBF-IV). In addition, a number of recent studies have taken advantage of the superior resolution of the *Hubble Space Telescope* (*HST*) for SBF measurements (Ajhar et al. 1997; Lauer et al. 1998; Neilsen & Tsvetanov 2000; Jensen et al. 2001) reaching as far as 10,000 km s<sup>-1</sup>. A recent comprehensive review of SBF is given by Blakeslee, Ajhar, & Tonry (1999a).

In this paper, we perform a series of comparisons between the SBF and FP distance methods. The following section describes the SBF and FP calibrations, distances, and Malmquist corrections, as well as the hybrid ‘ $\overline{N}$ SBF’ distance estimator and distances predicted using the line-of-sight distance-redshift relations derived from the observed *IRAS* galaxy density field. The FP distances use photometric parameters derived by Blakeslee et al. (2001a, hereafter Paper I) from the SBF survey data images and velocity dis-

persions from the SMAC survey. Section 3 performs a series of direct comparisons between the distances obtained by the different methods for individual galaxies. Section 4 discusses potential systematic biases in the distance methods, particularly in regard to the Hubble flow, or alternatively, the value of the Hubble constant, implied by the early-type galaxy distance scale. The final section summarizes our main results.

## 2 THE DISTANCES

The present work intercompares three types of galaxy distances: SBF measurements, FP measurements, and distances predicted from the observed galaxy density field. The predicted distances are used mainly for investigating potential problems in the SBF-FP comparison. We give an overview of these three types of distance estimation before directly comparing the distances.

### 2.1 SBF Distances

#### 2.1.1 ( $V-I$ )-calibrated SBF

We use the data from the ground-based SBF survey as tabulated by SBF-IV. The distances are calculated from the measured  $I$ -band apparent fluctuation magnitude  $\overline{m}_I$  and the  $(V-I)_0$  colour according to

$$\overline{M}_I = -1.74 + 4.5 [(V-I)_0 - 1.15] \quad (1)$$

$$(m - M) = (\overline{m}_I - \overline{M}_I) \quad (2)$$

(Tonry et al. 2000, hereafter SBF-II). The colour dependence is based on the behavior of  $\overline{m}_I$  among galaxies in groups, and the zero point is based on SBF measurements in the bulges of six spirals for which Cepheid distances have been measured. Problems and uncertainties in this empirical calibration are discussed in Appendix B of SBF-II. The Cepheid distances are those tabulated by Ferrarese et al. (2000) for the *HST* Key Project on the Distance Scale. The total uncertainty in the  $\overline{M}_I$  zero point is about 0.2 mag and is dominated by systematic effects, such as the LMC distance. For a discussion of the theoretical SBF calibration and uncertainty from stellar population modeling, see Liu et al. (2000) and Blakeslee et al. (2001b).

Freedman et al. (2001) have recently updated the Key Project distances using the revised Cepheid P-L relation from Udalski et al. (1999) (although keeping the LMC distance modulus at 18.50 mag) and the metallicity correction from Kennicutt et al. (1998). The effects of these two changes on the distances to the SBF calibrating spirals nearly cancel. The resulting SBF direct calibration would be about 0.06 mag fainter, well within the uncertainty of Eq. (1).

We adopt the SBF distance errors from SBF-IV, which are 0.22 mag in the median, but we add an allowance for uncertainty in the Galactic extinction values from Schlegel, Finkbeiner, & Davis (1998, hereafter SFD). This is important because extinction errors cause the SBF and FP distances to go in different directions. Because of the steep colour-dependence of  $\overline{M}_I$ , an underestimate of the true extinction produces an underestimate of the SBF distance:  $\pm \delta(m - M)_{\text{SBF}} = \pm 3.8 \delta E(B-V)$ , where we have used Eq. (1) and the extinction ratios recommended by SFD.

For the FP and most other distance indicators, underestimating the extinctions produces overestimated distances:  $\pm\delta(m-M)_{\text{FP}} = \mp 2.6\delta E(B-V)$ , in the  $R$  band. SFD concluded that the error on a given extinction value was 16% of the value, i.e.,  $|\delta E(B-V)| = 0.16 E(B-V)$ . This implies a distance error from extinction of  $0.61 E(B-V)$  for  $(V-I)_0$ -calibrated SBF and  $0.42 E(B-V)$  in the opposite sense for  $R$ -band FP, or  $\sim 1.0 E(B-V)$  for the difference. Therefore, the agreement will be worse in areas of high extinction; conversely, it is usually possible to bring the FP and SBF distances for any given galaxy at high extinction into agreement by changing the extinction estimate.

### 2.1.2 $\bar{N}$ -calibrated SBF

SBF-IV introduced an alternative calibration for SBF based on the distance-independent fluctuation count  $\bar{N}$ , defined as

$$\bar{N} = \bar{m} - m_{\text{tot}} = +2.5 \log \left[ \frac{L_{\text{tot}}}{\bar{L}} \right], \quad (3)$$

where  $m_{\text{tot}}$  and  $L_{\text{tot}}$  are the total apparent magnitude and luminosity of a galaxy and  $\bar{L}$  is the luminosity corresponding to magnitude  $\bar{m}$  at the distance of the galaxy. SBF-IV derived the following empirical calibration based on this new parameter:

$$\bar{M}_I = -1.74 + 0.14(\bar{N} - 20.0). \quad (4)$$

The distance modulus is then given by

$$(m - M) = 0.86 \bar{m}_I + 0.14 m_{\text{tot},I} + 4.54. \quad (5)$$

Thus, the distance moduli are 14% less sensitive to errors in  $\bar{m}_I$  and the goal of a  $\lesssim 0.02$  mag uncertainty in  $(V-I)$  is replaced by that of a  $\lesssim 0.6$  mag uncertainty in the total magnitude. Moreover, the moduli are about 50% less sensitive to the Galactic extinction and are affected in the sense opposite to how they are affected when using the  $(V-I)_0$  calibration of Eq. (1).

However, use of  $\bar{N}$  removes one of the most attractive features of SBF, its pure basis in stellar populations. The validity of the calibration relies on the universality of early-type galaxy scaling relations, in particular the mass-metallicity relation (e.g., Guzmán et al. 1992; Bender, Burstein, & Faber 1993). Although Blakeslee et al. (2001b) showed how composite population models combined with scaling relations can produce a tight relation involving  $\bar{m}$  and  $m_{\text{tot}}$ , the  $\bar{N}$ -based SBF method cannot be calibrated in a purely theoretical way.

Most importantly for the present work, the use of  $\bar{N}$  introduces strong covariance between the SBF and FP distances, as the value of  $m_{\text{tot}}$  used for  $\bar{N}$  is strongly correlated with the FP photometric combination  $X_{\text{FP}} \equiv \log R_e - \beta \langle \mu \rangle_e$  (see §2.2). Figure 1 shows the correlation: at fixed  $\bar{m}_I$ , the SBF distance modulus determined from  $\bar{N}$  goes as  $\sim 0.6 X_{\text{FP}}$ . This covariance produces a tight correlation and a non-unit slope for the relation between  $\bar{N}$ -derived  $(m-M)_{\text{SBF}}$  and  $(m-M)_{\text{FP}}$ , making the results difficult to interpret. SBF-IV and Paper I also showed good correlations between  $\bar{N}$  and  $\log \sigma$ , which essentially reflects the scaling of velocity dispersion with the total number of stars in a galaxy. Although comparisons between ' $\bar{N}$  SBF' and FP distances are therefore not meaningful, we *can* compare the  $\bar{N}$  SBF distances to those predicted from the *IRAS* density

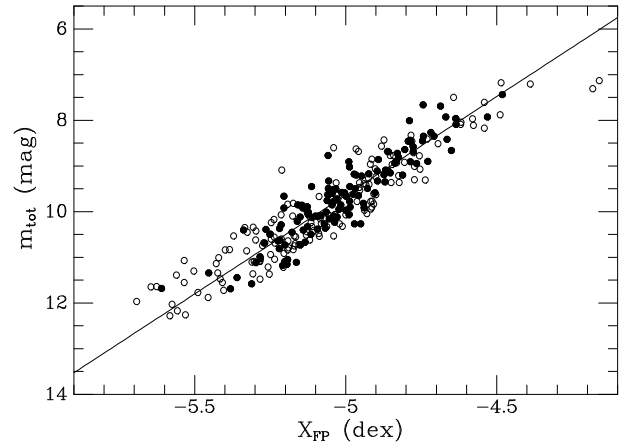


**Figure 1.** Illustration of the covariance between the estimated total apparent magnitude  $m_{\text{tot}}$  and the FP photometric parameter  $X_{\text{FP}} \equiv \log R_e - 0.33 \langle \mu \rangle_e$ . Filled circles are for  $T = -5$  ellipticals; open circles are other galaxies. The solid line is a least-squares fit to the ellipticals; the slope is 4.3. The two open circles falling below the line at the extreme right are the Local Group compact elliptical M32 and the nearby spiral M81, neither of which are used for any of the distance comparisons below.

field and see how the agreement changes with respect to the standard  $(V-I)_0$ -calibrated SBF distances.

## 2.2 FP distances

The FP relation can be represented as

$$\log R_e = \alpha \log \sigma + \beta \langle \mu \rangle_e + \gamma. \quad (6)$$

If the distance is known by other means, so that  $R_e$  is measured in physical units (kpc) then  $\gamma$  is a constant. More commonly,  $R_e$  is measured in angular units, so that determination of  $\gamma_i$  for an individual galaxy or cluster yields the angular diameter distance  $d_{A,i}$  relative to some calibrating cluster of known angular diameter distance  $d_{A,0}$  and zero point  $\gamma_0$ :

$$d_{A,i} = d_{A,0} 10^{(\gamma_0 - \gamma_i)}. \quad (7)$$

One then solves the angular distance equation (we use  $q_0 = 0$ , but this is unimportant for the present sample) to obtain the Hubble distance, i.e., the redshift  $cz$  the galaxy would have if its peculiar velocity were zero.

When  $\gamma_i$  is determined from a fit that minimizes the residuals in the distance-dependent quantity  $\log R_e$ , the method is known as the 'forward' FP; when residuals are minimized in  $\log \sigma$ , it is the 'inverse' FP. Of course, it is also possible to perform a fit minimizing the scatter orthogonal to the plane (e.g., Jorgensen et al. 1996). For any given galaxy, the forward FP provides the best estimate of the distance, as long as the fit coefficients have been determined from an unbiased sample (which is the difficult part). The inverse FP reduces selection biases for magnitude- or diameter-limited cluster galaxy samples at different distances (Schechter 1980), but does not yield the 'best distance' for any given galaxy. Strauss & Willick (1995) give a detailed discussion of the relative merits of the forward and inverse methods.

Colless et al. (2001) tabulate values of  $\alpha$  and  $\beta$  (actually  $B \equiv 2.5\beta$ ) from 9 different FP studies over the last decade.

The values of  $\beta$  show good consistency, having a range from 0.316 to 0.348, with an average of 0.326 and a dispersion less than 0.01. The SMAC survey determined a best fit value  $\beta = 0.338$ . We fix  $\beta = 0.33$ , or  $B = 0.825$ , as used for the  $X_{\text{FP}}$  comparisons of Paper I. This is very close to the coefficients derived from very large data samples by Hudson et al. (1997), Jorgensen et al. (1996), Colless et al. (2001) and the SMAC project.

The best-fitting  $\alpha$  will depend on whether one does a forward, inverse, or orthogonal fit to the FP. The SMAC survey used the inverse FP and derived  $\alpha = 1.42$ . Forward and orthogonal fits give smaller values; for example, Jorgensen et al. (1996) obtained  $\alpha = 1.24 \pm 0.07$ . Although we are using SMAC data, we are interested in comparing FP and SBF distances to individual galaxies, unlike SMAC, which was a cluster survey. Thus, we use the forward form of the relation derived from the Coma cluster, for which the SMAC data set is about twice as large as for any other cluster.

Because of the selection effect called ‘diameter bias’ by Lynden-Bell et al. (1988), the slope  $\alpha$  of the forward fit to a magnitude-limited sample will be too shallow and the zero point too high. Cutting the sample at progressively higher values of  $\log \sigma$  yields steeper slopes up to  $\log \sigma \sim 2.1$ , at which point  $\alpha = 1.22 \pm 0.09$ . Figure 2 shows the relation and a fit to the data with  $\log \sigma \geq 2.15$  ( $\sigma_{\text{cut}} = 140 \text{ km s}^{-1}$ ) and the moderate outlier D-120 excluded. The rms scatter is 0.064 dex (0.073 dex including D-120) in  $X_{\text{FP}}$ , or 0.32–0.37 mag, implying a  $\sim 17\%$  distance error per galaxy. The FP distance error for cluster galaxies is typically about 20% (see the compilation by Colless et al. 2001). For the adopted  $\alpha = 1.22$  and  $\log \sigma > 2.15$ , the  $R$ -band Coma FP zero point is  $\gamma_{\text{Com}} = -8.377 \pm 0.009$ .

Finally, we note that these values of  $\alpha$  are measured in the  $R$  band, and  $\alpha$  may depend on the bandpass. The main evidence for this comes from the result  $\alpha = 1.53 \pm 0.08$  found by Pahre et al. (1998) from an orthogonal fit to the  $K$ -band FP, as compared to the significantly shallower slope found by Jorgensen et al. (1996) and others. However, the data samples and analyses methods also differ among these studies. In contrast, Girardi et al. (in preparation) have derived the FP of a homogeneous sample of 9000 galaxies in the Sloan  $g'r'i'z'$  bands and find no significant variation in  $\alpha$  among these bands for a given type of FP fit.

### 2.3 Inhomogeneous Malmquist Corrections

Malmquist (1920) investigated the luminosity bias in flux-limited samples and the resulting distance error which occurs near the sample limit when assuming all the objects have the same luminosity. Here, we use ‘Malmquist bias’ as in the terminology of Lynden-Bell et al. (1988) to refer to the distance bias arising from the spatial distribution of the sample galaxies, including the increase in the volume element with distance. We note that this differs from the selection biases referred to by the same name by Schechter (1980), Aaronson et al. (1986), and others (see Strauss & Willick 1995 for details). By ‘inhomogeneous Malmquist bias’ we mean the apparent tendency of galaxies to be scattered out of regions of higher density by the observational errors. As shown by Hudson (1994), correcting for this bias is especially important when treating early-type galaxies as field galaxies. In particular, Hudson found that inhomogeneous

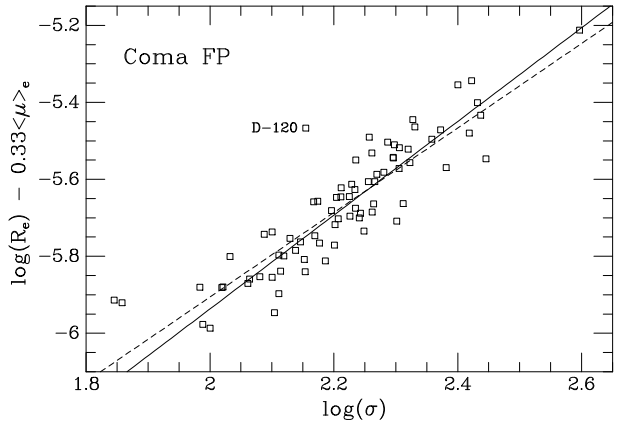


**Figure 2.** The ‘forward’  $R$ -band FP for galaxies in the Coma cluster with SMAC data. The effective radii  $R_e$  are in arcseconds, the surface brightness  $\langle \mu \rangle_e$  are in mag arcsec $^{-2}$ , and the velocity dispersions  $\sigma$  are in km s $^{-1}$ . The dashed line is a least-squares fit to the full sample of 76 galaxies; its slope of 1.10 is too shallow because of incompleteness at small values of  $X_{\text{FP}}$  ( $X_{\text{FP}}$  is biased high at small values of the velocity dispersion  $\sigma$  because of selection effects). The solid line is a fit to the 54 galaxies with  $\log \sigma \geq 2.15$  and has a slope of 1.22. This fit is used to define the forward SMAC FP. The galaxy D-120 (labelled) was omitted from the fit, but the slope is not very sensitive to this.

Malmquist bias was largely responsible for previous claims of ‘backside’ infall into the Great Attractor (e.g., Dressler & Faber 1990).

We essentially follow Strauss & Willick (1995) in correcting for inhomogeneous Malmquist bias. This approach forms the basis of the VELMOD maximum likelihood method used by Willick et al. (1997) and Willick & Strauss (1998) to constrain the properties of local mass density field from galaxy peculiar velocities measured with the Tully-Fisher method. In particular, they constrained the density parameter  $\beta_I \equiv \Omega^{0.6}/b_I$ , where  $b_I$  is the linear biasing factor of the *IRAS* 1.2 Jy survey (Fisher et al. 1995) galaxies with respect to the mass density field and  $\Omega$  is the mean cosmic density. The VELMOD method was also applied to the SBF survey peculiar velocities by Willick & Batra (2001).

In the notation of Strauss & Willick, an unbiased estimate of the true distance  $r$  for a galaxy of measured distance  $d$  is given by the expectation value

$$E(r|d) = \frac{\int_0^\infty r^3 n(r) \exp\left\{-\frac{[\ln(r/d)]^2}{2\Delta^2}\right\} dr}{\int_0^\infty r^2 n(r) \exp\left\{-\frac{[\ln(r/d)]^2}{2\Delta^2}\right\} dr}, \quad (8)$$

where  $n(r)$  is the real-space galaxy density distribution in the direction of the given sample galaxy,  $\Delta$  is the fractional distance error, and the errors are assumed Gaussian in log distance. Note that because it goes as  $n(r)r^2$ , the distance probability tends to have a tail to larger distances. This means that the unbiased distance  $E(r|d)$  tends to be larger than the maximum-probability distance, which is usually closer to the measured  $d$ . For the case of a uniform density, Eq. (8) yields the Lynden-Bell et al. (1988) homogeneous Malmquist correction factor of  $e^{3.5\Delta^2}$ .

We estimate  $n(r)$  and derive the redshift-distance relation along the line of sight to each of our sample galaxies

using the redshift distribution of the *IRAS* 1.2 Jy survey under the assumptions of linear theory, a linear biasing model with  $\beta_I = 0.4$ , and a power-preserving filter with a smoothing scale of 300 km s $^{-1}$  (see Willick et al. 1997 and Willick & Strauss 1998 for details). The comparisons of the Malmquist-corrected FP and SBF distances are not very sensitive to the value of  $\beta_I$  adopted. However, Blakeslee et al. (1999b, hereafter SBF-III), using the spherical harmonic expansion method of Nusser & Davis (1994), found that the comparison between SBF survey peculiar velocity measurements and the *IRAS* density field predictions implied  $\beta_I = 0.42^{+0.10}_{-0.06}$ , and Riess et al. (1997) found  $\beta_I = 0.40 \pm 0.15$  using the same method but SNIa peculiar velocities. Willick & Batra (2001), whose methods and ‘*IRAS* model’ we have largely adopted for this analysis, found  $\beta_I = 0.38 \pm 0.06$ , again using SBF survey peculiar velocities.

One difference with respect to Willick & Batra is that we do not directly insert  $n(r)$  determined from the *IRAS* galaxies into Eq. (8), where the relevant density distribution is that of the early-type galaxies in our sample. Instead, we write the early-type galaxy density as

$$n_e(r) = 1 + \frac{b_e}{b_I} \delta_I(r), \quad (9)$$

where  $\delta_I(r)$  is the relative overdensity of the *IRAS* galaxies and  $b_e$  and  $b_I$  are the biasing factors of the early-type and *IRAS* galaxies, respectively. Baker et al. (1998) found the relative biasing between optically-selected ( $R$  band) and *IRAS* galaxies to be  $\frac{b_e}{b_I} \approx 1.4$ , while Willmer et al. (1998) and Narayanan, Berlind, & Weinberg (2000) found  $\frac{b_e}{b_I} \approx 1.2$  for the relative biasing of early-types and spirals. If early-type galaxies make up 10–50% of optically selected galaxies, the relative biasing factor of early-type to *IRAS* galaxies is then 1.5–1.6. We adopt  $\frac{b_e}{b_I} = 1.5$ , although the results of the analysis would change very little for ratios in the range 1.0–1.7, and use Eq. (9) for the density in Eq. (8).

## 2.4 Distances from the Density Field

The peculiar velocity predictions from the observed galaxy density field provide a third set of distances for the galaxies in our sample. These predictions are usually compared to the observed peculiar velocities in order to constrain  $\beta_I$ , and thus  $\Omega$ . Here, we are mainly interested in having an independent set of distances for evaluating the SBF–FP comparisons, and so we simply adopt the *IRAS* model described above. Again, following Willick & Batra (2001), the expectation value of the true distance  $r$  for an observed redshift  $cz$  along a given line of sight is

$$E(r|cz) = \frac{\int_0^\infty r^3 \frac{n(r)}{\sigma_v(r)} \exp\left\{-\frac{(cz-[r+u(r)])^2}{2\sigma_v^2(r)}\right\} dr}{\int_0^\infty r^2 \frac{n(r)}{\sigma_v(r)} \exp\left\{-\frac{(cz-[r+u(r)])^2}{2\sigma_v^2(r)}\right\} dr}, \quad (10)$$

where  $\sigma_v$  is the thermal noise in the velocity field and  $u(r)$  is the radial component of the predicted peculiar velocity. We allow the thermal noise for this early-type SBF galaxy sample to vary with local *IRAS* galaxy density as

$$\sigma_v(r) = [185 + 15\delta_I(r)] \text{ km s}^{-1} \quad (11)$$

(Willick, private communication). To estimate the error  $\delta r$  in the predicted distance, we calculate  $E(r^2|cz)$  analogously to Eq. (10) and then

$$\delta r = \sqrt{E(r^2|cz) - [E(r|cz)]^2}. \quad (12)$$

The actual errors in the *IRAS*-predicted distances may be greater than this in general, as the adopted model will not be a perfect description of the density field and non-linear effects can be significant.

In calculating the predicted distances, we use the observed galaxy velocities (transformed to the Local Group frame) except in a few cases where there are known very large peculiar velocities. For Virgo, we set all 16 sample galaxies within 5° of M87 and local group velocity  $v_{\text{LG}} < 2700$  km s $^{-1}$  to have  $v_{\text{LG}} = 1035$  km s $^{-1}$  and  $\sigma_v = 50$  km s $^{-1}$ . The Eridanus group galaxy NGC 1400 has a relative velocity of  $-1215$  km s $^{-1}$  with respect to NGC 1407, a larger elliptical at a projected separation of only  $63 h^{-1}$  kpc. We simply change the velocity of NGC 1400 to be that of NGC 1407. In Centaurus, a variety of evidence, including colour-magnitude relations and luminosity functions (Lucey, Currie, & Dickens 1986), the optical  $D_n-\sigma$  relation (Lucey & Carter 1988), the near-infrared FP (Pahre et al. 1998), and high resolution SBF observations from *HST* Cycle 6 (discussed in SBF-II), indicates that the ‘Cen-30’ and ‘Cen-45’ ellipticals lie at the same physical distance. Thus, we reassign the 3 Cen-45 galaxies in our sample to have  $v_{\text{LG}} = 2935$  km s $^{-1}$  (for a CMB velocity  $v_{\text{CMB}} = 3500$  km s $^{-1}$ ).

These predicted distances and the SBF distances both could be used to derive the FP coefficients from the sample galaxies directly, without using the SMAC Coma cluster data. For two reasons we have elected not to do this. First, we wish to look for possible systematic problems or trends in the distance comparisons, and so it is best to keep the different types of distances independent. Second, we are also interested in the value of  $H_0$ , so we wish to tie as directly as possible the Cepheid-calibrated distances (in Mpc) from SBF to the Hubble flow-calibrated distances (km s $^{-1}$ ) from the FP and *IRAS*. For illustration, however, Figure 3 shows the *IRAS*-calibrated FP of our sample galaxies. The best-fitting slope for the galaxies with  $\log \sigma > 2.1$  is  $1.11 \pm 0.11$  ( $1.05 \pm 0.07$  for the full sample), consistent with the Coma slope. The rms scatter is 0.12 dex (0.11 dex for the ellipticals), which includes the errors in the estimated distances. However, the best agreement with the Coma zero point is achieved if Coma has a CMB-frame peculiar velocity of about  $+1000$  km s $^{-1}$ . We discuss the results of the distance comparisons in greater detail below.

## 3 COMPARISON OF DISTANCES

We matched all galaxies beyond the Local Group having SBF distances (distance modulus uncertainty  $< 0.7$ ) against all galaxies with FP distances constructed from SMAC velocity dispersions and SBF survey photometry (Paper I). There are a total of 170 galaxies in this cross-matched sample. Of these, we omit 6 galaxies from the  $\chi^2$  analyses for the following reasons. Three galaxies (NGC 404, NGC 4476, and NGC 4489) have velocity dispersions  $\sigma < 50$  km s $^{-1}$  (no others have  $\sigma < 70$  km s $^{-1}$ ) and thus would have very uncertain FP distances. One galaxy (NGC 3641, a close companion of

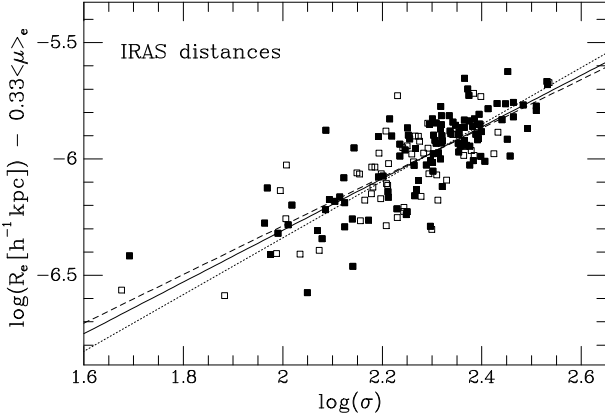


**Figure 3.** The ‘forward’ FP for galaxies in the present cross-matched sample of SBF–SMAC galaxies. The distances used in transforming the  $R_e$  values to a common scale ( $h^{-1}$  kpc) are those derived from the *IRAS* redshift survey density field as described in the text. The dashed line (with a slope of 1.05) and the solid line (with slope 1.11) show the linear fits to the full and  $\log \sigma > 2.1$  samples, respectively, and the dotted line shows a fit to the  $\log \sigma > 2.1$  sample for a fixed slope of 1.22, as for the Coma FP. Solid and open symbols represent ellipticals and S0s, respectively, but the fits shown are to all galaxies regardless of type; restricting the fit to ellipticals produces virtually identical results.

the much brighter NGC 3640) has an FP distance over 7000  $\text{km s}^{-1}$ , even though its velocity is only  $\sim 2000 \text{ km s}^{-1}$ ; it is  $\sim 5.5\sigma$  outlier in both the FP-SBF and FP-*IRAS* comparisons. Two galaxies (NGC 2305 and E322-059, also called NGC 4645A) have exceptionally poor SBF data with quality parameters  $\text{PD} > 3.6$  (see §4.2 below for the definition of PD) and probably biased distance estimates as a result. Both are  $\sim 3\sigma$  outliers in the FP-SBF comparisons, but NGC 2305 is  $5.8\sigma$  outlier in the SBF-*IRAS* comparison because it is in a region of the sky where the predicted error on the *IRAS* distance is very small (0.11 mag). Note that this is the only data-quality cut we make (and we still plot these galaxies in the comparison figures below), as we wish to explore the possibility of bias in the poorest quality SBF survey data, an issue raised in SBF-II where a much more severe PD cut was made to avoid any potential selection bias. We are left with 164 galaxies for judging goodness of fit for the distance comparisons. Of the 6 rejected, only 2 are big outliers (NGC 3641 in the FP-SBF and FP-*IRAS* comparisons and NGC 2305 in the SBF-*IRAS* comparison), although all six are strongly suspected of systematic problems.

Figure 4 plots the FP distances against the SBF distances. For the FP distances, we have assumed a Hubble velocity of  $7355 \text{ km s}^{-1}$  (the best-fitting SMAC value) for Coma and the FP zero point found in §2.2. With these assumptions, we find that  $H_0 \approx 68 \text{ km s}^{-1} \text{ Mpc}^{-1}$  minimizes  $\chi^2$  for this distance comparison, and have adopted this value for the figure. The distances have been corrected for inhomogeneous Malmquist bias as described in the previous section; the small covariance introduced by using the same density field for these corrections is ignored (different errors go into the corrections). The agreement in Figure 4 is generally good, although the scatter is larger for the 53 S0s (0.70 mag, or 0.65 mag excluding the one  $> 2$  mag outlier) than

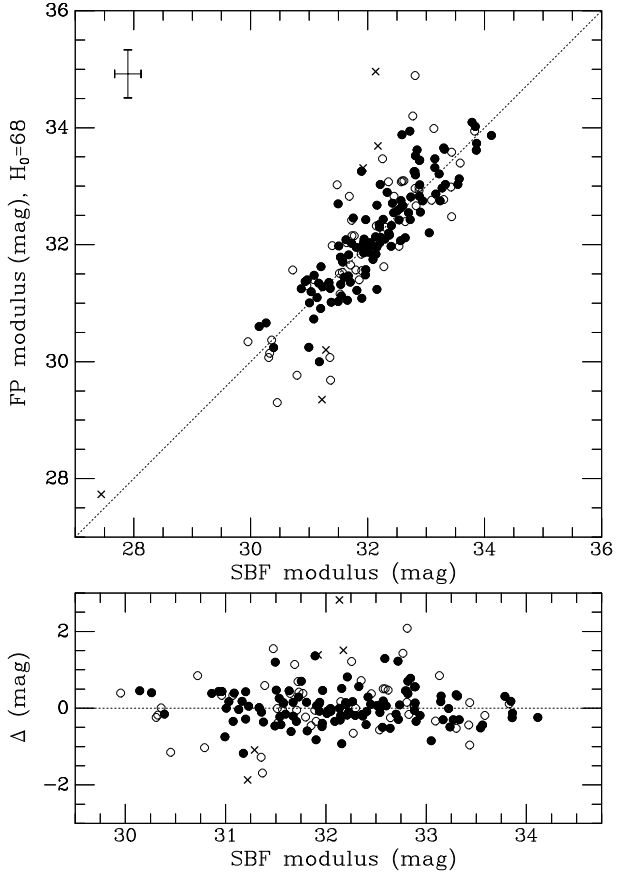


**Figure 4.** Comparison of the Malmquist-corrected FP and SBF distance moduli for the 170 galaxies in the cross-matched sample. The upper panel shows the direct comparison, and the lower panel shows the residuals (FP modulus minus SBF modulus) with an expanded horizontal axis. The FP distances are converted to Mpc using the best fitting  $H_0$  for this comparison. The median errors are indicated at upper left, but note that the SBF distances do not all have the same error. The dotted lines indicate equality, and are not fits to the points. The different symbols represent ellipticals (filled circles), S0s (open circles), and the six galaxies excluded from our  $\chi^2$  fits (crosses). Of the six excluded galaxies, four have velocity dispersions that are either very low ( $\sigma < 70 \text{ km s}^{-1}$ ) or apparently in error (NGC 3641), and thus have suspect FP distances; two have very poor quality SBF observations ( $\text{PD} = 3.6$ ) which apparently bias the distances. The four nearby, non-excluded S0s with  $\Delta(\text{FP} - \text{SBF}) < -1.0$  mag, in order of increasing  $(m-M)_{\text{SBF}}$ , are NGC 3489 (Leo I?), NGC 6684, NGC 4382 (Virgo), and NGC 1553 (Dorado).

for the 111 ellipticals (0.45 mag), where we define the ellipticals as having a morphological  $T$ -type of  $-5$  in the RC3 (de Vaucouleurs et al. 1991).

The larger scatter for the S0s is mainly due to a group of particularly low-luminosity galaxies with  $(m-M)_{\text{SBF}} \approx 31.0$  but  $(m-M)_{\text{FP}} \approx 29.7$ . The S0s cause an apparent trend for the residuals  $\Delta(m-M)_{\text{FP-SBF}}$  to increase with distance. This is made more clear in Figure 5, which plots the residuals against the *IRAS*-predicted distances and the CMB-frame velocities. The trend of increasing  $\Delta(m-M)_{\text{FP-SBF}}$  with  $(m-M)_{\text{IRAS}}$  is formally significant at 95% confidence for the full sample but only 42% confidence (i.e., not significant) for just the ellipticals.

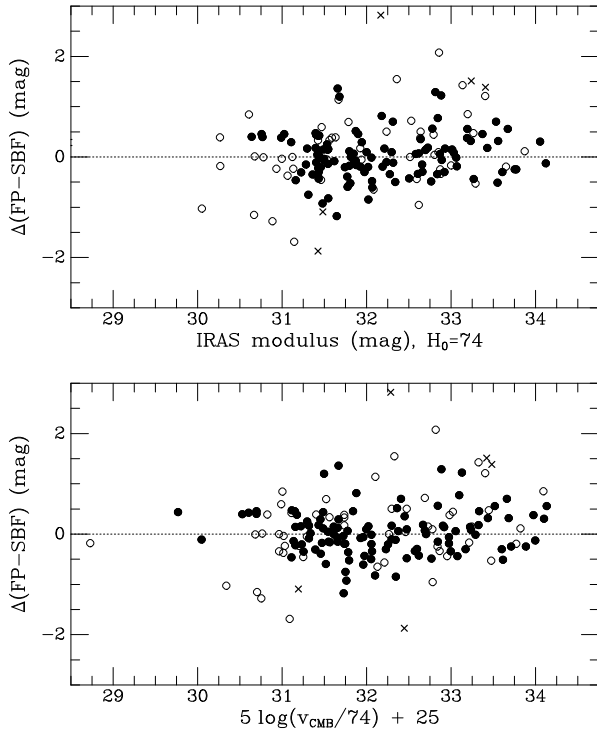


**Figure 5.** The residuals of the FP-SBF distance comparison are plotted against *IRAS*-predicted distance modulus (top) and CMB-frame velocity converted to a distance modulus (bottom). The value of  $H_0 = 74$  used for the horizontal axis is unimportant, as different values would simply shift all the points uniformly. Symbols are as in Figure 4.

Table 1 gives more information on this and subsequent distance comparisons, including comparisons for the following subsamples: ellipticals, galaxies with  $v_{\text{CMB}} \leq 3000 \text{ km s}^{-1}$ , galaxies with  $(V-I)_0 > 1.135$  and intersections of these. It includes the number of galaxies for the comparison, the best-fitting value of  $H_0$  and the reduced  $\chi^2$  for each comparison, and the formal slope and reduced  $\chi^2$  for a bivariate linear fit of, for example, FP distance versus SBF distance. These results are discussed in greater detail in the following section on systematic effects.

In calculating the values of  $\chi^2$  (and thus the best-fitting  $H_0$ , etc), we used the errors described above for the SBF and *IRAS* distances, and a fixed 19.0% distance uncertainty for the FP, which nominally includes an intrinsic scatter of 18% and a 7% distance error from  $X_{\text{FP}}$  uncertainties (Paper I). Overall, the FP distance error would have to be 21.7% to give  $\chi^2_{\nu} \equiv 1$  for the FP-SBF comparison, assuming the SBF errors are accurate, but this neglects the obvious problems with some S0s. For just the 111 ellipticals, a distance error of 17.6% would give  $\chi^2_{\nu} \equiv 1$ .

Figures 6 and 7 plot the FP and SBF distances against the *IRAS* distances, and Table 1 again summarizes the results. It would of course be possible to plot all galaxies with SBF or FP distances against the *IRAS*-predicted distances, but our intent was to use the *IRAS* distances as a tool for diagnosing the problems and biases in the FP-SBF distance comparisons. Previous work (SBF-III; Willick & Batra 2001) have made comparisons of the *IRAS* predictions with the full SBF survey data set. Figure 6 shows that the same problem

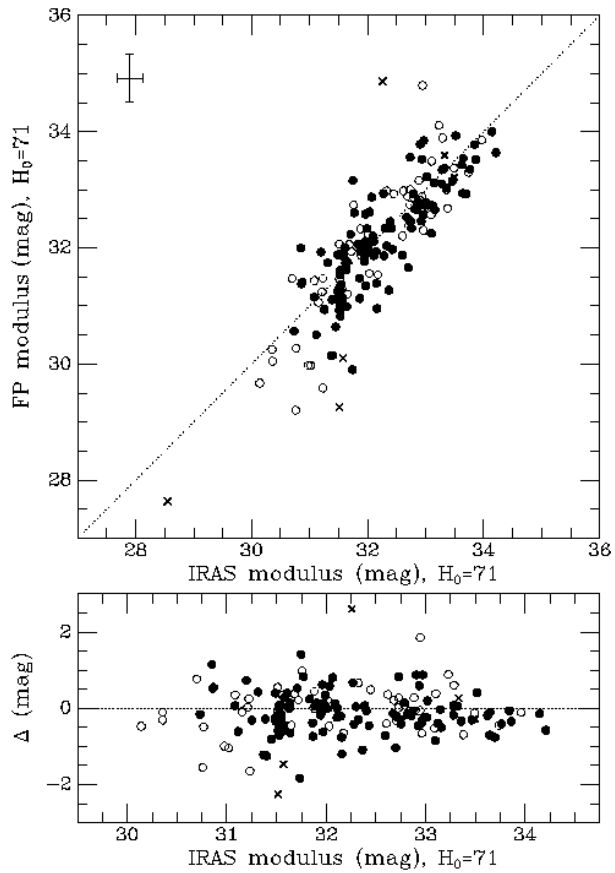


**Figure 6.** Same as Figure 4 but for the FP-*IRAS* distance comparison.

with the nearby S0s occurs in the FP-*IRAS* comparison as in the FP-SBF comparison, and this causes the slope of the FP versus *IRAS* distances to be  $2\sigma$  greater than unity for the full sample. As one might expect given that a fixed FP distance error was used for all galaxy types,  $\chi^2_{\nu}$  decreases for the FP-*IRAS* comparison when only the ellipticals are considered. Yet, it unexpectedly increases by 10% when this is done for the SBF-*IRAS* comparison. Five of the six galaxies that are more than  $2\sigma$  discrepant in this comparison are ellipticals. It is possible that the peculiar velocities of the ellipticals are more prone to small-scale non-linear effects and that the smoothing of the density field underpredicts the local overdensity, or that ellipticals preferentially occupy regions of non-trivial biasing with respect to the *IRAS* density field. For such situations, Eq. (11) would become inadequate. The poorer FP distances for the S0s would hide this effect in the FP-*IRAS* comparison. We plan to address this issue more fully in a future paper.

As noted in §2.1.1 above, comparisons between the hybrid  $\bar{N}$ -calibrated SBF distances and the FP distances would be misleading and difficult to interpret because of the strong covariance between  $X_{\text{FP}}$  and  $m_{\text{tot}}$ . However, we can compare the  $\bar{N}$  SBF distances with those predicted from the *IRAS* density field, as shown in Figure 8. Because the intrinsic scatter in the  $\bar{m}_I - m_{\text{tot}}$  relation is not well characterized, and we do not have an extensive set of homogeneous external  $m_{\text{tot}}$  values to gauge our accuracy, we simply adopt

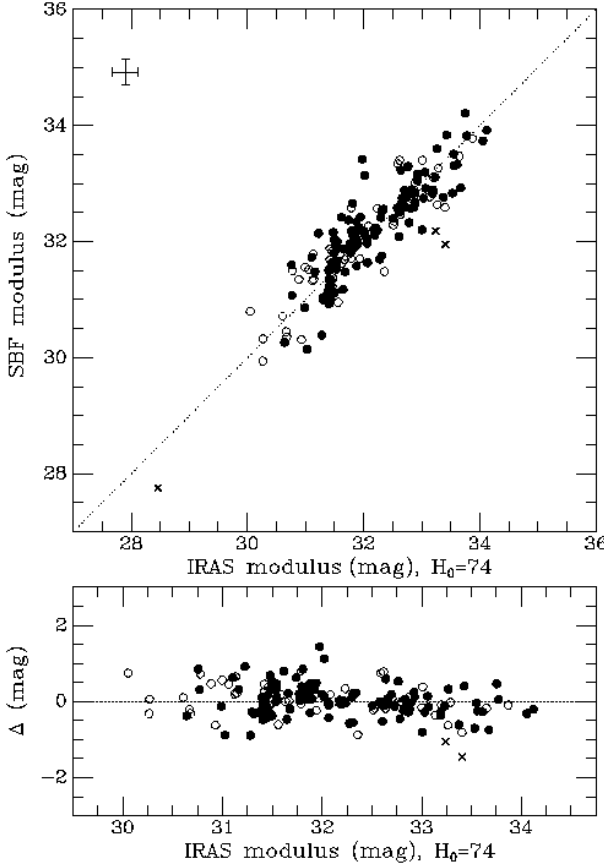


**Figure 7.** Same as Figure 4 but for the SBF-*IRAS* distance comparison.

the same error for the  $\bar{N}$  SBF distances as for the  $(V-I)_0$ -calibrated SBF distances, except we leave out the contribution from reddening. This simplifies the intercomparison of  $\chi^2$  from the two analyses.

Surprisingly, the  $\bar{N}$  calibration of SBF actually improves the agreement with *IRAS* over that achieved with the usual  $(V-I)_0$  calibration. The scatter in Figure 8 is 0.36 mag for the S0s and 0.38 mag for the ellipticals, as compared to 0.40 mag and 0.41 mag, respectively, in Figure 7. Tables 1 shows the improvements in  $\chi^2_\nu$ . This reflects how hard it is to determine  $(V-I)_0$  to sufficient accuracy (including the correction for Galactic reddening) as well as the decreased sensitivity to  $\bar{m}_I$  errors (Eq. 4).

Figure 9 shows the sky distribution of the distance modulus residuals for the three sets of distance comparisons, where the SBF distances are calibrated using  $(V-I)_0$ . For comparison to the SBF distances, the FP and *IRAS* distances are converted to Mpc using the respective best-fitting values of  $H_0$ . This type of residual plot emphasizes the outliers by showing them with larger symbols; the six galaxies excluded from the  $\chi^2$  analyses for the reasons given above are not shown here. Positive (circles) and negative (crosses) residuals appear fairly well mixed in all three panels of Figure 9, indicating that there are no major direction-dependent systematic errors in the three sets of distance estimates.

Overall, the different distance indicators agree quite

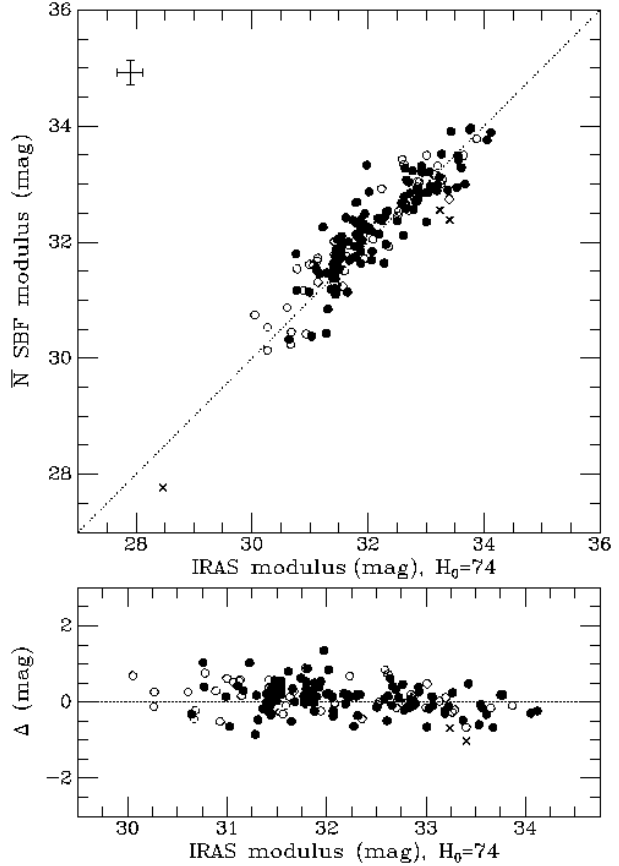


**Figure 8.** Same as Figure 4 but for the  $\bar{N}$ -calibrated SBF-*IRAS* distance comparison.

well and are consistent within the errors so that the comparisons yield  $\chi^2_\nu \sim 1$ . The good agreement allows us to discern possible systematic problems in the data. We explore this issue in greater detail in the following section.

## 4 DISCUSSION

### 4.1 The Velocity Field and $\beta_I$

Figure 10 shows the dependence of the reduced  $\chi^2$  and best-fitting  $H_0$  values from the different comparisons of Table 1 on the CMB-frame velocity limit. The  $\chi^2_\nu$  values for the different comparisons are very stable against the velocity cut. However, there does appear to be some tendency for  $H_0$  to increase for  $v_{\text{CMB}} \gtrsim 3000 \text{ km s}^{-1}$ , which is significant at the  $1-2\sigma$  level; a possible explanation is discussed in the following section. Perhaps the most striking aspect of Figure 10 is that although there is a  $\sim 30\%$  improvement in  $\chi^2_\nu$  when the SBF-FP comparison is restricted to ellipticals, the inferred  $H_0$  changes by less than 2%.

Figure 11 plots  $\chi^2_\nu$  and  $H_0$  from the same comparisons against the value of  $\beta_I$  used for the velocity field reconstruction and the density term in the Malmquist corrections. Figure 12 is the same, but restricted to galaxies with  $v_{\text{CMB}} < 3000 \text{ km s}^{-1}$ . The SBF-FP comparison shows reassuringly little dependence on  $\beta_I$ . The lower panels of Figures 11 and 12 indicate that  $H_0$  from the SBF-*IRAS* com-

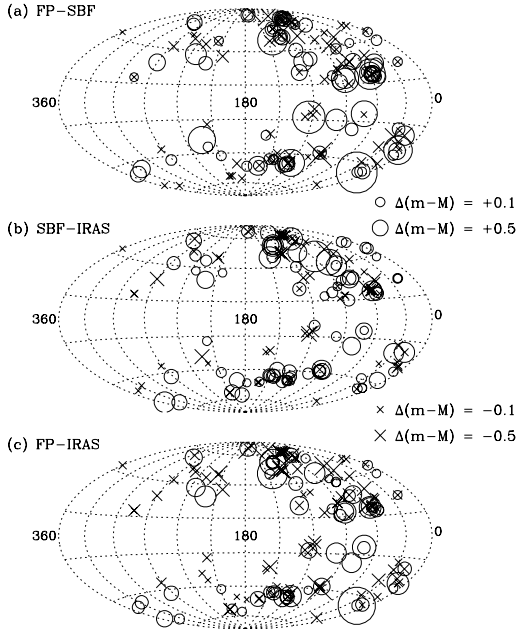


**Figure 9.** Sky distribution (Aitoff projection) of the distance modulus residuals in Galactic coordinates for the three sets of distance comparisons: (a)  $(m-M)_{\text{FP}} - (m-M)_{\text{SBF}}$  for  $H_0 = 68 \text{ km s}^{-1} \text{ Mpc}^{-1}$ , (b)  $(m-M)_{\text{SBF}} - (m-M)_{\text{IRAS}}$  for  $H_0 = 74 \text{ km s}^{-1} \text{ Mpc}^{-1}$ , and (c)  $(m-M)_{\text{FP}} - (m-M)_{\text{IRAS}}$ . Circles show positive residuals and crosses show negative residuals. Symbol size is proportional to  $[0.5 + |\Delta(m-M)|]$ , so that zero residuals are shown as circles of finite radius.

parison can be brought into agreement with that from the SBF-FP comparison for  $\beta_I \approx 0.1$ . However, the SBF-IRAS comparison strongly rejects values of  $\beta_I < 0.3$ , as do most other analyses of this sort, which typically give  $\beta_I$  in the 0.4–0.9 range (e.g., da Costa et al. 1998; Willick & Strauss 1998; Riess et al. 1997; Sigad et al. 1998; Hudson et al. 1999). Thus, there is little prospect for reducing the disagreement on  $H_0$  to less than 9%.

There appears to be little constraint on larger values of  $\beta_I$  from these data if  $H_0$  is allowed to increase in tandem, and the constraints are weakened when restricted to  $v_{\text{CMB}} < 3000 \text{ km s}^{-1}$ . However, when high-quality data at large distance from *HST* are introduced, the covariance between  $H_0$  and  $\beta_I$  is reduced and the constraints are strengthened. SBF-III concluded that the  $1\sigma$  uncertainty on  $H_0$  from  $\beta_I$  itself, and thus the IRAS-velocity tie, was only about 1.5%. However, this does not include possible systematic errors in the IRAS redshift sample used in deriving the density field; see §4.6 below.

#### 4.2 Selection Bias in the SBF Survey?

SBF-II discussed a possible bias in the SBF survey data, such that the poorest quality data preferentially produced systematically low distance estimates. The main data-quality indicator they used was PD, which is the product of the seeing full-width at half-maximum in arcseconds and the CMB frame velocity in units of  $1000 \text{ km s}^{-1}$  (so  $[\text{PD}]^2$

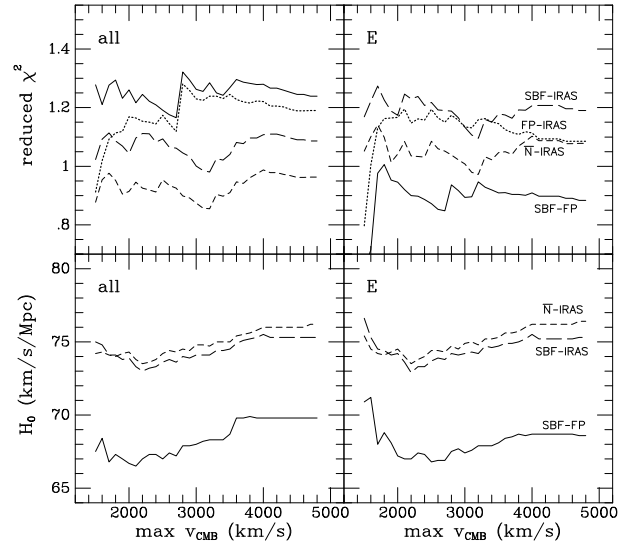


**Figure 10.** The reduced  $\chi^2$  (top panels) and the best-fitting  $H_0$  values (lower panels) for the various distance-distance comparisons are shown as a function of the cutoff CMB frame velocity for the comparisons. The comparisons are labelled. Left panels show results from the full sample regardless of morphological type; right panels show the results when the sample is restricted to ellipticals.

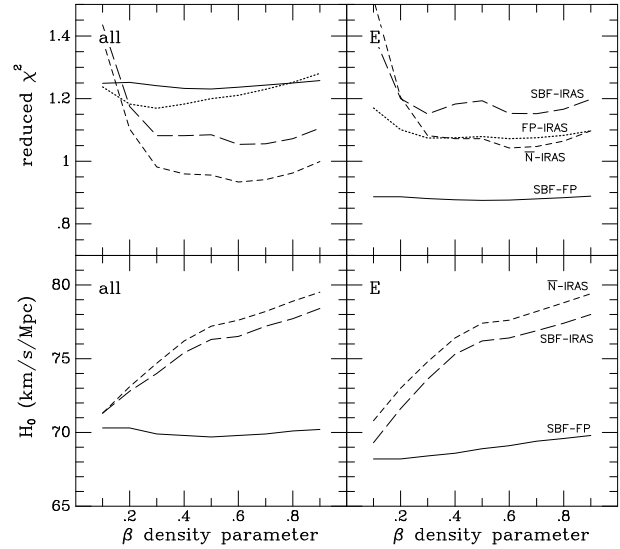


**Figure 11.** The reduced  $\chi^2$  (top panels) and the best-fitting  $H_0$  values (lower panels) for the various distance-distance comparisons are shown as a function of the IRAS  $\beta$  parameter used in the galaxy density field reconstruction and peculiar velocity predictions. Left panels show the results for all morphological types; right panels show the results when the sample is restricted to ellipticals. The SBF-FP comparisons are insensitive to  $\beta$  because the density field is only used for the inhomogeneous Malmquist corrections to these distances, but it is the basis of the IRAS-predicted distances. No velocity restriction was applied to the galaxies for these comparisons.

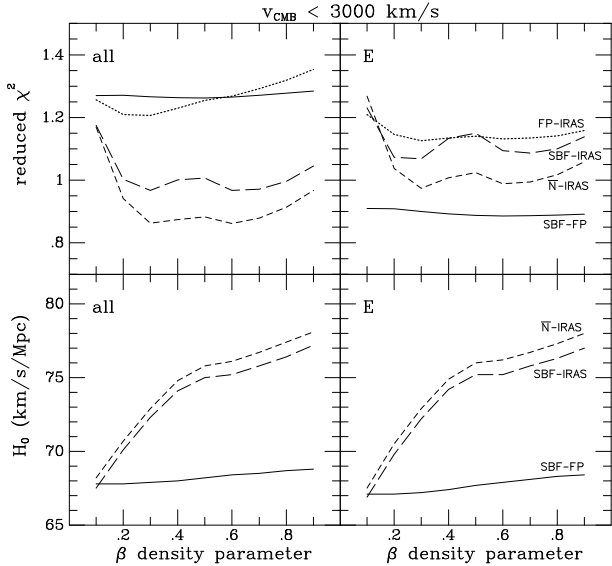


**Figure 12.** Same as Figure 11 except the comparisons have been restricted to galaxies with CMB frame velocities  $v_{\text{CMB}} < 3000 \text{ km s}^{-1}$ .

goes as the metric area within a resolution element). Occasionally, repeat observations with high values of PD  $\sim 3$  gave erroneously low distances. Because of this perceived ‘PD bias,’ SBF-II used only data with PD  $< 2.7$  for their analysis, and SBF-III adopted the same PD-cutoff. SBF-IV included results for observations with  $2.7 < \text{PD} < 3.0$  in a separate table for ‘uncertain SBF data.’

A bias in the poorest quality data is reasonable to expect if the SBF survey is viewed as  $\bar{m}$ -limited. Near the  $\bar{m}$  limit of the survey, if the SBF signal is not detected (inferred distance too big) the galaxy does not make it into the catalogue, but if the SBF is detected (inferred distance smaller), it does make it in. Galaxies with the largest true distances in the survey will have measured distances that are too low, because their true  $\bar{m}$  values will be fainter than the survey limit, and observational error has scattered them into the survey catalogue (these might be called ‘spurious SBF detections’). This selection bias at the faint limit of the survey is distinct from the Malmquist bias which occurs at all distances (although both biases are rooted in normal observational error and are minimized when these errors are small).

Because the exposure times and seeing conditions of the SBF observations were tailored to the expected distances of the galaxies, the survey data are not actually  $\bar{m}$ -limited, but we should still expect this sort of selection bias in marginal SBF detections. The only way to avoid it would be to volume-limit the sample with a conservative cutoff, or to impose a volume limit as a function of the seeing in the data image. Effectively, this is what the PD  $< 2.7$  cutoff of SBF-II and SBF-III did: impose a volume limit of  $2700 \text{ km s}^{-1}$  for  $1''$  seeing and allow this limit to scale with seeing so that it was about Virgo distance for  $2''$  images and  $\sim 4000 \text{ km s}^{-1}$  for the best ( $0''.65$ – $0''.7$ ) seeing.

As seen in Figures 5 and 7, there may be some evidence for a bias in the SBF distances at the largest ‘true’ distances (gauged by CMB velocity or *IRAS*-predicted distance). This

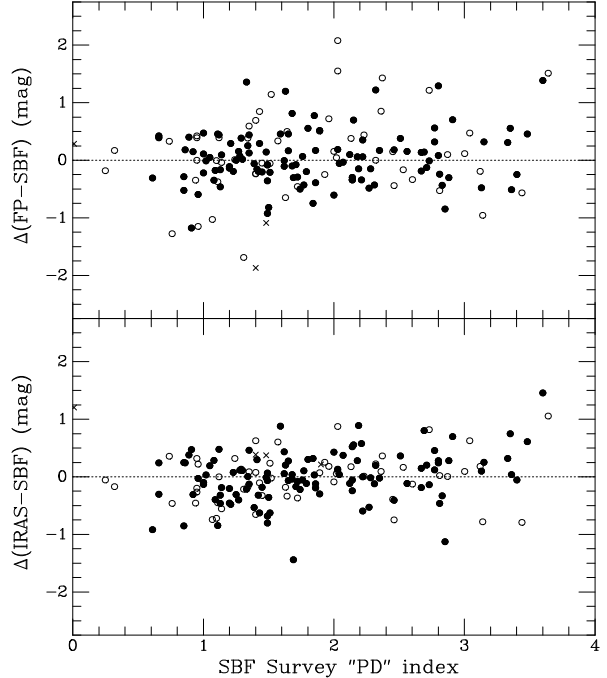


**Figure 13.** The difference between the FP and SBF distance moduli (top) and *IRAS*-predicted and SBF distance moduli (bottom) are plotted against the SBF data quality index PD from SBF-II. The symbol types are as in Figure 4, except there is no need to distinguish the two (apparently biased) PD  $> 3.5$  galaxies with crosses here.

effect is also seen in the increasing inferred  $H_0$  for increasing  $v_{\text{CMB}}$  cutoffs in Figure 10. However, the overall slope (no distance or velocity limit) of a bivariate fit to the SBF-*IRAS* distance modulus comparison is unity,  $1.00 \pm 0.03$  (Table 1). The slope for a bivariate of the full SBF-FP comparison is  $3\sigma$  from unity, but this is largely driven by the nearest S0s; when the S0s are excluded, the slope is within  $1\sigma$  of unity.

Figure 13 shows the residuals of the FP-SBF and SBF-*IRAS* comparisons as function of PD. As plotted, the residuals will be preferentially positive at large PD if there is a significant selection bias. It appears that the PD  $> 2.7$  selection bias in the SBF survey data is not as bad as feared by SBF-II. This may be because SBF-II did not correct for Malmquist bias, which, although distinct from the selection bias, increases with PD because the observational errors do. Figure 14 illustrates this point. Consequently, any bias parameterized by PD will be a combination of Malmquist and selection biases and will be reduced following Malmquist correction. That said, there remains a suggestion of SBF selection bias in the SBF-*IRAS* comparison of Figure 13: 11 of 14 galaxies, including 7 of 8 ellipticals, with PD  $> 3.0$  have positive residuals, and the two with PD  $\approx 3.6$  may well be ‘spurious SBF detections.’ However, it is important to note that the data with PD  $> 3.0$  were judged as too poor to be included even in the ‘uncertain data’ table of SBF-IV. We conclude that, following the inhomogeneous Malmquist corrections applied here, SBF data with PD  $< 3$  show very little evidence of selection bias.

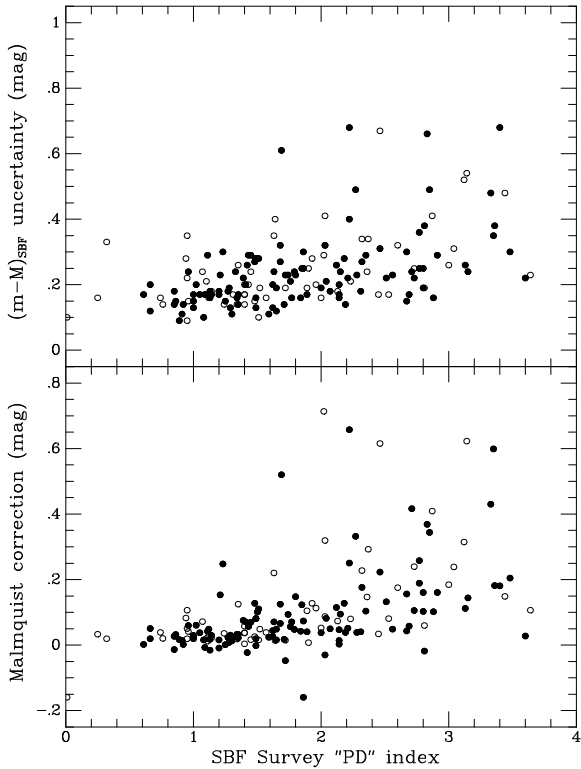


**Figure 14.** The SBF survey distance uncertainties (top) and the inhomogeneous Malmquist bias corrections determined in Section 2.3 are plotted as a function of the PD data quality index from SBF-II. Open symbols are for ellipticals and filled symbols are for S0s. The Malmquist corrections increase with PD because the poorer quality data have larger errors on average.

#### 4.3 Stellar Population Effects

The SBF method makes an explicit correction for stellar population in terms of  $(V-I)_0$  colour. The FP method, as applied here and in most other works, assumes that all early-type galaxies of a given mass have essentially the same stellar population, i.e., that the mass-to-light ratio scales in a consistent way with mass. Variations in the stellar content, such as from recent star formation, will cause deviations from the FP at some level. Here, we examine the possibility of trends in the distance residuals with  $Mg_2$  index and  $(V-I)_0$  colour.

Figure 15 plots the residuals of the FP-SBF, FP-*IRAS*, and SBF-*IRAS* distance comparisons against  $Mg_2$ . Overall, the trend of increasing  $\Delta(m-M)_{\text{FP-SBF}}$  with  $Mg_2$  is significant at the  $3.7\sigma$  level, or  $2.3\sigma$  for the ellipticals and  $3.6\sigma$  for the S0s. The trend of increasing  $\Delta(m-M)_{\text{FP-IRAS}}$  with  $Mg_2$  is significant at  $2.2\sigma$ , or  $2.0\sigma$  for the ellipticals and  $2.8\sigma$  for the S0s. These trends appear to be real, but mild and not subject to simple interpretation. There is no significant trend in the SBF-*IRAS* distance residuals with  $Mg_2$ .

Because  $Mg_2$  correlates so strongly with  $\log \sigma$ , these trends may simply reflect sample selection effects, and not indicate a problem with the individual distances. For instance, the slope  $\alpha = 1.22$  determined from the Coma cluster was used for the FP distances even though it does not give the formal (naive) ‘best fit’ to the FP of our more inhomogeneous sample. The shallower slopes of  $\alpha \approx 1.0\text{--}1.1$  (e.g., Figure 3) found by calibrating the FP for the current

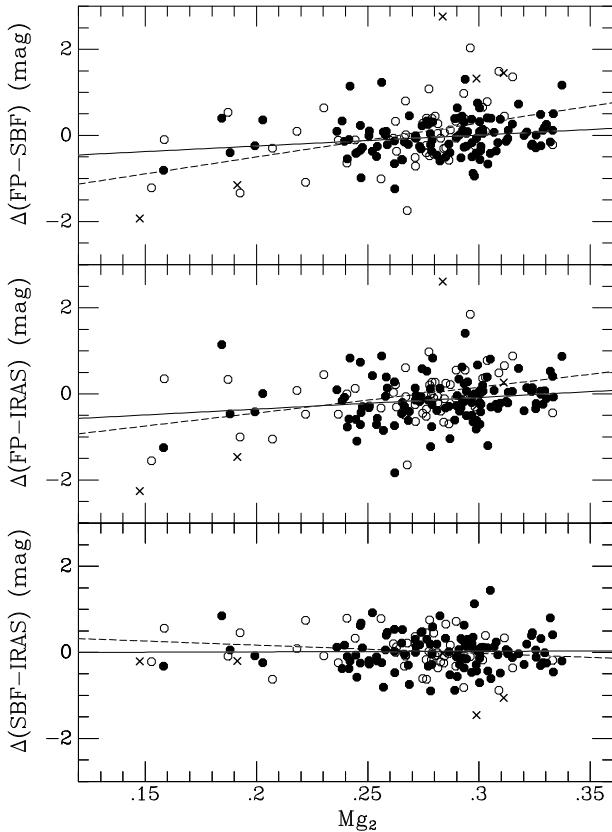


**Figure 15.** The differences between the FP and SBF distance moduli (top), FP and *IRAS*-predicted moduli (middle), and SBF and *IRAS*-predicted moduli (bottom) are plotted against  $Mg_2$ . The symbol types are as in Figure 4. Solid and dashed lines are simple least-squares fits to the elliptical and S0 subsamples, respectively (not to the combined sample).

sample using SBF and *IRAS* distances would decrease the significance of the trends with  $Mg_2$  to  $\sim 2.8\sigma$  for FP-SBF and  $\sim 1.8\sigma$  for FP-*IRAS*, but we avoided these shallower slopes because they are determined from an inherently biased sample.

Figure 16 illustrates the situation, showing that the luminosity-based sample selection causes the mean  $\log \sigma$  and  $Mg_2$  to increase with distance. What we should test for then is some systematic trend of the  $Mg_2$ – $\log \sigma$  residuals with distance, to see if stellar population effects are causing a distance-dependent bias in the FP distance estimates. We assume the  $Mg_2$ – $\log \sigma$  relation found in Paper I. As the bottom panel of Figure 16 indicates, we find no significant overall trend of the residuals with distance. The slope of the residuals with  $v_{\text{CMB}}$  is within  $\sim 0.6\sigma$  for the full sample and the elliptical subsample (for which the best-fitting slope actually goes in the opposite sense).

For the S0 subsample (again, including the  $T = -4$  extended cD galaxies), the slope deviates from zero by  $1.8\sigma$ . However, this is mainly the result of a few outliers. The largest positive residual is NGC 3311 at  $v = 4200 \text{ km s}^{-1}$ . In fact, this galaxy well illustrates the power of the fundamental plane. NGC 3311 is a massive, extended, low central surface brightness cD in Hydra; its velocity dispersion is only  $\sigma = 190 \text{ km s}^{-1}$ , which is consistent with the low  $\langle \mu \rangle_e$ ,

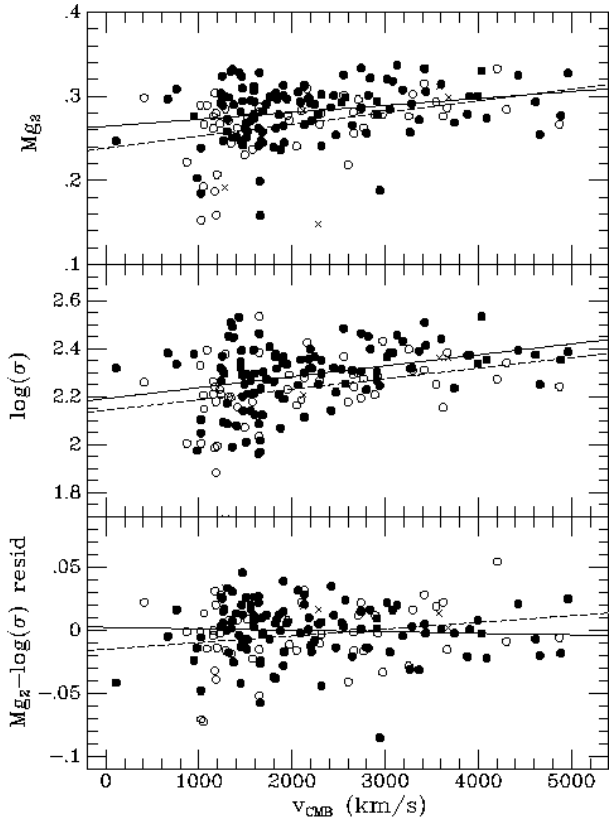


**Figure 16.**  $Mg_2$  (top),  $\log \sigma$  (middle), and residuals with respect to the mean  $Mg_2$ – $\sigma$  relation from Paper I (bottom) are plotted against CMB-frame velocity. The residuals in the bottom panel are positive (negative) when the observed  $Mg_2$  is greater (lower) than the predicted value from the mean relation and the observed  $\log \sigma$ . Symbol types are as in Figure 4. Solid and dashed lines are simple least-squares fits to the elliptical and S0 subsamples, respectively (not to the combined sample).

but causes a deviation from the  $Mg_2$ – $\log \sigma$  relation because the central dispersion is not a good indicator of mass for this galaxy. We also note that NGC 3311 has some dust in its centre, although this appears confined to radii  $\lesssim 5''$ , much smaller than the effective radius  $R_e \approx 100''$ . In any case, the dust would not affect the galaxy’s position in Figure 16, and does not cause any significant discrepancy between its SBF and FP distances, which agree to within  $0.5\sigma$ .

On the other hand, the two most significant negative residuals at  $1000\text{ km s}^{-1}$  (NGC 3489, NGC 4382) are nearby S0s having FP distances significantly smaller than the SBF or *IRAS* distances; thus, these galaxies do deviate from the FP, and they deviate because their velocity dispersions are too low for their luminosities (causing underestimated FP distances). The excess luminosity could result from recent star formation, which would decrease their  $Mg_2$  below the value expected at a given  $\log \sigma$ , consistent with Figure 16. We conclude that the few nearby S0s which cause the weak trend in  $Mg_2$ - $\log \sigma$  with redshift deviate from the general relation, at least in part, because of their stellar populations, although anomalous virial properties for low-mass S0s could contribute. In addition, errors in their  $\log \sigma$  aperture corrections may also play a role (see §4.5).

For comparison to the  $Mg_2$  plots, Figure 17 plots the

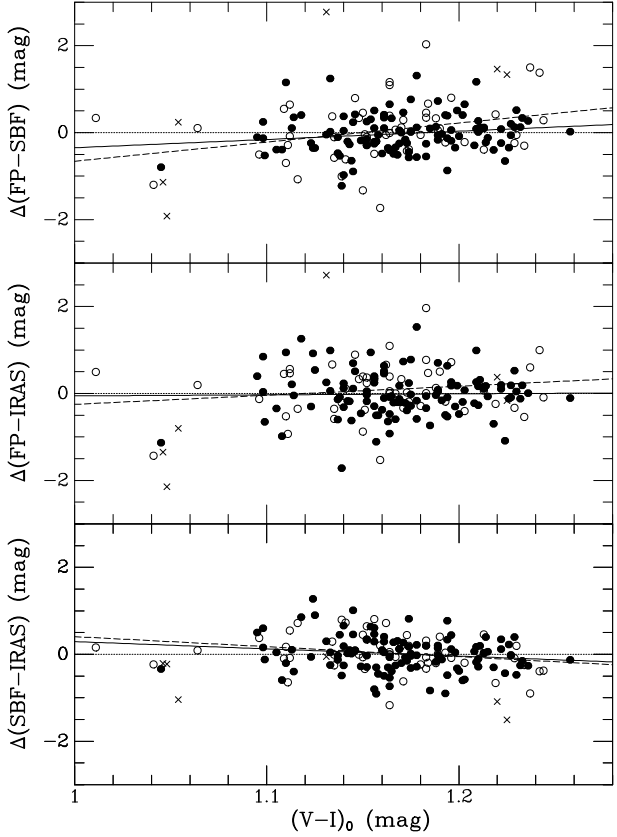


**Figure 17.** Distance residuals for the FP-SBF, FP-*IRAS*, and SBF-*IRAS* comparisons are plotted against  $(V-I)_0$  colour. Symbol types are as in Figure 4. Solid and dashed lines are simple least-squares fits to the elliptical and S0 subsamples, respectively (not to the combined sample).

distance residuals against  $(V-I)_0$  colour. The only trend that is significant at more than  $2\sigma$  here is the increase of  $\Delta(m-M)_{\text{FP-SBF}}$  with  $(V-I)_0$ , which is  $3\sigma$  significant for the full sample and S0 subsample,  $2\sigma$  significant for the elliptical subsample. There are two reasons for this trend: first, the nearby galaxies with the underestimated FP distances tend to be blue; second, and similar to the above case for the FP and the shallower best-fitting slope against  $\log \sigma$ , this sample would call for a naive best-fitting slope for  $\overline{M}_I$  versus  $(V-I)_0$  that is somewhat shallower than the 4.5 found from the maximum likelihood analysis of galaxies in groups by SBF-I. In any case, the trend of the SBF-*IRAS* residuals with  $(V-I)_0$  is not significant at the  $2\sigma$  level.

It is noteworthy that, if anything, the bluer galaxies in Figure 17 tend to have underestimated FP distances; this would not be the case if the negative  $X_{\text{FP}}$  residuals found in the comparison to the Faber et al. (1989) data by Paper I had resulted from a bias in our fits to the SBF survey photometric data. If that were the case, our FP distances for these galaxies would be biased high, but there is no evidence of that here. The reduced  $\chi^2$  values for the distance comparisons do improve when the bluer galaxies are excluded (Table 1), but again, this is because the nearby galaxies with underestimated FP distances are mainly blue S0s.

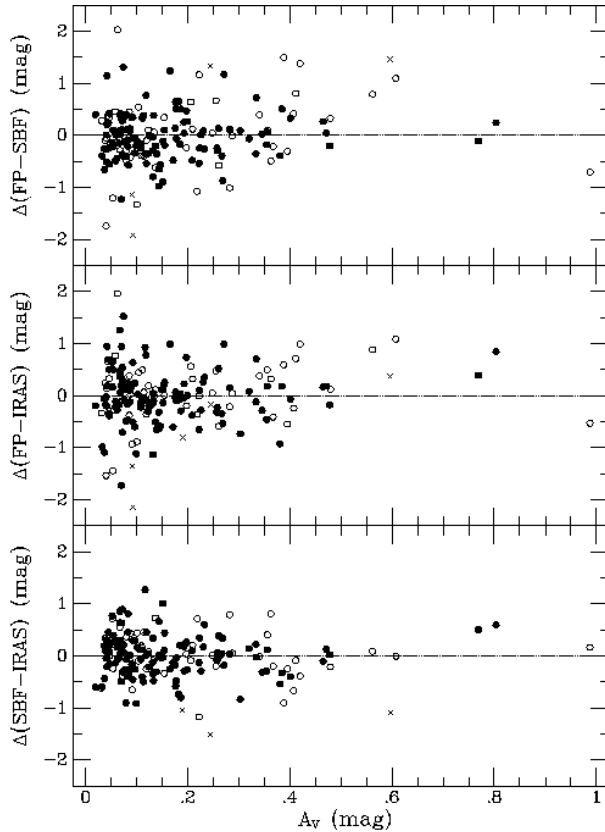


**Figure 18.** Distance residuals for the FP-SBF, FP-IRAS, and SBF-IRAS comparisons are plotted against  $V$ -band extinction from SFD. Symbols are as in Figure 4.

#### 4.4 Galactic Extinction

Figure 18 plots distance residuals against  $A_V$  extinction from SFD. As noted in §2, the SBF distance will be overestimated, while the FP distance underestimated, if the extinction is overestimated, and vice versa. The distances predicted by the *IRAS* flux-limited survey should be essentially independent of SFD extinction errors, or at least related in a nontrivial way. While it is intriguing that the S0s with  $A_V \gtrsim 0.4$  mag tend to have larger FP than SBF or *IRAS* distances, if this were an effect of extinction errors, these galaxies would all have to have a true  $A_V$  very close to zero, which is unlikely. In short, we find no evidence for a dependence of the residuals on  $A_V$ , but the distance errors are too large for a very significant test. Better constraints on extinction errors can be found from the residuals of the Mg<sub>2</sub>-colour relation (e.g., SFD; Hudson 1999; Paper I).

#### 4.5 Aperture Effects

The SMAC survey estimated aperture corrections for the velocity dispersion data using

$$(\log \sigma)_{\text{cor}} = (\log \sigma)_{\text{obs}} + 0.04 \log \left( \frac{r_{\text{ap}}}{r_{\text{norm}}} \right), \quad (13)$$

where the normalization radius  $r_{\text{norm}}$  is the angular size corresponding to  $0.6 h^{-1}$  kpc and  $r_{\text{ap}}$  is the radius of a circular aperture equivalent to the spectroscopic extraction aperture. The logarithmic slope of 0.04 is taken from Jorgensen et al.

(1995), who used an extensive set of empirical models to derive mean aperture corrections. These authors quoted a FWHM for the logarithmic slope distribution of 0.06 (0.01–0.07) and found a weak correlation of the slope with  $\log \sigma$  such that a mean of  $\sim 0.03$  was more appropriate for low dispersion galaxies and  $\sim 0.05$  was more appropriate for high dispersion ones.

Our FP measurements are tied to the Coma cluster, which is  $\sim 8$  times more distant than the closest galaxies in the present survey, yet the galaxies in our sample had their dispersions measured in apertures not much larger than used for Coma. Aperture corrections therefore have the potential for being a significant source of systematic error, and one which we have not yet considered. We wish to address the following two questions. First, could aperture effects be the cause of the apparently underestimated distances for some of the nearby, low-dispersion galaxies? This includes the S0s listed in the caption to Figure 4 and the two galaxies at a similar distance which were excluded (and shown as crosses in the distance comparison figures) specifically because of their low dispersions. Second, how large is the systematic uncertainty in the tie to the Coma cluster, and therefore the value of  $H_0$ , resulting from the aperture corrections?

For the nearby discordant galaxies, the aperture correction given by Eq. (13) for  $r_{\text{ap}} \approx 2''$  (see SMAC-III) amounts to about 0.035 dex in  $\log \sigma$ , or about 10% in distance. The assumed logarithmic slope for  $\log \sigma$  needs to be decreased for the nearby low-dispersion galaxies in order to increase their distances, and this is qualitatively consistent with the assertion by Jorgensen et al. (1995) that these galaxies have shallower  $\log \sigma$  profiles. However, even if we took a slope of 0.0, indicating no gradient, their distances would be increased by only 0.2 mag, not the  $\sim 1$  mag required to bring these galaxies into agreement with the SBF and *IRAS* distances in Figures 4 and 6. Therefore, while inappropriate aperture corrections may contribute to the discrepancy for these galaxies, the full explanation likely involves stellar population effects as well (§4.3).

With regard to  $H_0$ , we note that the median redshift of the galaxies in the sample is about  $1800 \text{ km s}^{-1}$ , implying a median aperture correction of 0.021 dex from Eq. (13), or a median correction to the distances of 6%. If we allow that the mean slope of the  $\log \sigma$  gradients for these galaxies may differ by  $\pm 0.015$  from the 0.040 used in the SMAC catalogue, which seems reasonable given the range found by Jorgensen et al. (1995), as well as the scatter in  $\log \sigma$  gradients observed by Franz et al. (1989), then the derived distance scale may change by 2.2%, or about  $\pm 1.5 \text{ km s}^{-1} \text{ Mpc}^{-1}$  in  $H_0$ . We use this in the following section in estimating the systematic uncertainty in  $H_0$ .

#### 4.6 Systematic Effects on $H_0$

The value of  $H_0$  found by tying the Cepheid-calibrated SBF distances to the Hubble flow via the FP is  $68.0 \pm 1.3$  from the ellipticals within  $3000 \text{ km s}^{-1}$  and all types within  $3000 \text{ km s}^{-1}$ , beyond which point  $H_0$  shows an increase that may reflect selection biases. The uncertainty in the Hubble-flow tie via the FP is about 3.5%, including a  $\sim 200 \text{ km s}^{-1}$  distance uncertainty for the peculiar velocity of the Coma cluster and the uncertainty due to aperture effects as described in the previous section. With an additional al-

lowance of 2.5% from half the range of  $H_0$  values from the various FP-SBF comparisons, we conclude  $H_0 = 68 \pm 3.2$   $\text{km s}^{-1} \text{Mpc}^{-1}$  from the SBF-FP comparison.

For the SBF-*IRAS* comparison, we adopt  $H_0 = 74 \pm 1.6$ , consistent with Table 1 (especially within 3000  $\text{km s}^{-1}$ ), but based also on the results and  $\beta_I$  uncertainty from SBF-III, which considered a total of 280 galaxies, including several observed with *HST*, and made a much more stringent  $\text{PD} < 2.7$  quality cut to avoid potential selection bias. Thus, the *IRAS* and FP ties of SBF to the far-field Hubble flow give  $H_0$  values differing by  $\sim 1.7\sigma$ . Another symptom of the problem, and one which does not involve SBF distances, is the large Hubble distance of  $\sim 8000$   $\text{km s}^{-1}$  for the Coma cluster given by the tie between the ‘*IRAS*-calibrated FP’ of Figure 3 and the observed Coma FP zero point in Figure 2. Note that the quoted errors on  $H_0$  include only the uncertainties on ties between the relevant methods.

These results are reminiscent of those of Willick & Batra (2001), who found that tying the Cepheid distances to the Hubble flow via the *IRAS* peculiar velocity predictions (which they called ‘Method 2’) gave an  $H_0 \sim 10\%$  greater than tying to the Hubble flow using the distance ladder of secondary indicators (‘Method 1’). The latter, Method 1, approach was used by the  $H_0$  Key Project group (e.g., Freedman et al. 2000; Gibson et al. 2000; Sakai et al. 2000; Freedman et al. 2001). (The other half of the  $\sim 20\%$  difference between the Key Project and Willick & Batra  $H_0$  values resulted from a systematic difference of nearly 0.2 mag in their Cepheid distance scales.)

The discrepancy seen here and by Willick & Batra could be explained if the *IRAS* redshift survey overestimates the density field locally, so that the local corrected velocities are systematically too high, yielding a higher  $H_0$ . This would result from a problem in the redshift survey completeness estimates as a function of distance. If this could be demonstrated, then we should prefer  $H_0 \approx 68$  from the FP-SBF comparison. However,  $H_0 = 74$  is only  $1.9\sigma$  from the best-fitting value from the SBF-FP tie, and could be closer to  $1\sigma$  if we had used slightly larger estimates of the systematic uncertainties. At this point, the safest bet might be a straight average of the two results,  $H_0 \approx 71 \pm 4$   $\text{km s}^{-1} \text{Mpc}^{-1}$ , where the  $1\sigma$  uncertainty is estimated from the difference over  $\sqrt{2}$ . This  $H_0$  is consistent with most other recent determinations from extragalactic distance indicators tied to the same Cepheid scale.

If we update the SBF zero point by  $+0.06$  mag according to the revised Key Project Cepheid distances from Freedman et al. (2001), then the Hubble constants from the FP-SBF and *IRAS*-SBF comparisons become 70 and 76  $\text{km s}^{-1} \text{Mpc}^{-1}$ , respectively. We estimate the systematic error from the 5% uncertainty in the tie between SBF and Cepheids (SBF-II), the  $\sim 10\%$  systematic uncertainty on the Cepheid distances (see for example Ajhar et al. 2001), and the additional  $\sim 10\%$  uncertainty in the LMC distance modulus (e.g., Walker 1999; Gibson 2000). Our final value for  $H_0$  from early-type galaxies calibrated against Cepheids is then  $H_0 = 73 \pm 4 \pm 11$   $\text{km s}^{-1} \text{Mpc}^{-1}$ .

We note that Freedman et al. (2001), based on the work of Kelson et al. (2000a), reported  $H_0 = 82 \pm 6 \pm 9$   $\text{km s}^{-1} \text{Mpc}^{-1}$  from the FP. However, they relied upon group association (the Cepheid distances to the Leo group and Fornax and Virgo clusters) for their distance calibration. In

addition, their calibrating and distant cluster samples (the latter being taken from Jorgensen et al. 1996) were observed in different bands, came from independent data sources, and had no photometric or spectroscopic overlap. Thus, while Kelson et al. provided detailed estimates of the systematic and random uncertainties, the true level of homogeneity between their calibrating and program samples was unknown. We believe our results for  $H_0$  are more robust for this reason.

## 5 SUMMARY AND CONCLUSIONS

We have used the  $X_{\text{FP}}$  photometric parameters derived for the SBF survey galaxies in Paper I and the homogenized velocity dispersions from SMAC-III to obtain FP distances for over half of the SBF survey galaxies. We corrected the FP and SBF distances for inhomogeneous Malmquist bias and intercompared the FP,  $(V-I)_0$ -calibrated SBF, and *IRAS*-predicted distances. The distance agreement was good overall, with reduced  $\chi^2$  values near unity for most of the comparisons. However, the inclusion of S0s significantly increases the scatter and  $\chi^2_{\nu}$  for the FP-SBF and FP-*IRAS* comparisons. While the mean error per FP measurement is found to be 21.7% overall, it is reduced to 17.6% when just ellipticals are considered. This is mainly due to the several nearby, low-dispersion, blue galaxies whose FP distances are anomalously low. For the SBF-*IRAS* comparison, the S0s actually decrease the scatter. While the reason for this is unclear, it may be that the smoothed *IRAS* velocity field model is simply inadequate for many ellipticals and underpredicts the local velocity field noise, so that the predictions for the S0s are more accurate overall.

We also compared the *IRAS* distances to SBF distances calibrated by the  $\bar{N}$  fluctuation count parameter introduced by SBF-IV. Because  $\bar{N}$  correlates strongly with the FP,  $\bar{N}$ -based distances can be considered a hybrid SBF-FP distance indicator; it is therefore not meaningful to compare  $\bar{N}$ -SBF and FP distances. We find the  $\bar{N}$ -SBF distances exhibit less scatter in the comparison to the *IRAS* distances. Taken at face value, the improvement in  $\chi^2$  indicates that the  $\bar{N}$ -SBF distances are roughly 25% more accurate than  $(V-I)_0$ -calibrated SBF distances. The better accuracy is due to the decreased sensitivity to photometric errors,  $\bar{m}$  measurement errors, and Galactic extinction.

In addition to the morphological effects, several other sources of potential systematic error were considered. These included the density parameter  $\beta_I$  used for the velocity reconstruction and the Malmquist corrections, selection biases in the SBF survey with distance, Galactic extinction, and stellar population and aperture effects. We found that low values of  $\beta_I \lesssim 0.1$  can bring the FP and *IRAS* ties to the Hubble flow into close agreement, but are excluded for other reasons. We find some evidence of selection bias near the limit of the SBF survey, seen in weak increases in  $H_0$  and in the reduced  $\chi^2$  for the SBF-*IRAS* comparison beyond about 3500  $\text{km s}^{-1}$ . However, this bias should not affect the published SBF survey distances or analyses, as these used fairly stringent quality cuts specifically to avoid this problem, whereas we have made essentially no quality cuts so that we could test for such a bias.

The nearby, blue, mainly S0 galaxies with underestimated FP distances are apparently affected by young stellar

populations, although possibly coupled with irregular virial properties and/or inappropriate aperture corrections. However, apart from these few nearby S0s, stellar population effects do not appear to significantly bias the FP distances. We also find no evidence that the Galactic extinction estimates contribute significant systematic distance errors.

The comparison between the Cepheid-calibrated SBF distances and the far-field Hubble flow calibrated FP distances yields  $H_0 = 68 \pm 3 \text{ km s}^{-1} \text{ Mpc}^{-1}$ , including statistical and systematic uncertainties in the SBF-FP tie and the tie of the FP distances to the Hubble flow. The SBF-*IRAS* comparison yields  $H_0 = 74 \pm 2 \text{ km s}^{-1} \text{ Mpc}^{-1}$ ; so, formally there is a  $\sim 1.7\sigma$  difference between  $H_0$  given by the two separate ties. However, additional sources of systematic error, such as larger uncertainties in the FP aperture corrections, or possible completeness errors in the *IRAS* density field used for the velocity reconstruction, would further reduce the marginal significance of this difference. Therefore, we have recommended a straight average of the above two  $H_0$  values. We have noted that the SBF distance zero point is from SBF-II, which uses the Key Project Cepheid distances tabulated by Ferrarese et al. (2000). Had we used a zero point based on the revised Cepheid tabulation by Freedman et al. (2001), the  $H_0$  values would be 2.8% greater. Therefore, the final average would be  $H_0 = 73 \pm 4 \text{ km s}^{-1} \text{ Mpc}^{-1}$  (internal error). Additionally, there is a systematic error of about 15% in  $H_0$  from the zero point of the Cepheid scale and the tie between SBF and Cepheids.

Future space-based SBF observations of ellipticals in a significant number of galaxy clusters should allow for further progress on the early-type galaxy distance scale. This will enable direct comparison of high-quality SBF distances to inverse FP measurements of cluster distances, each based on ten or more galaxies. Such a comparison would be much less sensitive to Malmquist, selection, and aperture biases. In addition, further *HST* SBF distances in the direction of the Hydra-Centaurus supercluster are greatly needed. The ground-based SBF survey do not sample this region well, and, as we have discussed, the galaxies are at a distance where there begins to be signs of selection bias. A detailed SBF investigation using *HST* would finally allow the complicated structure and dynamics of this important nearby region to be uncovered. Finally, we note that the zero point of the early-type galaxy distance scale will be improved by forthcoming *HST* measurements of Cepheid distances to late-type galaxies physically associated with ellipticals. This will secure our understanding of the physical structure of the Local Supercluster and tighten the constraints on  $H_0$  from early-type galaxies.

## ACKNOWLEDGMENTS

We thank our SBF and SMAC survey collaborators Ed Ajhar, Roger Davies, Alan Dressler, David Schlegel, and Russell Smith for their enormous efforts in these projects. We are grateful for enlightening email exchanges and encouragement from Jeff Willick early in this project. Despite his many responsibilities and commitments, Jeff was never too busy to share the benefits of his knowledge and experience. This work was supported at the University of Durham by a PPARC rolling grant in Extragalactic Astronomy and Cos-

mology and made use of Starlink computer facilities. JPB thanks the ACS project at Johns Hopkins University for support while finishing this paper.

## REFERENCES

Aaronson, M., Bothun, G., Mould, J., Huchra, J., Schommer, R. A. & Cornell, M. E. 1986, *ApJ*, 302, 536

Ajhar, E. A., Lauer, T. R., Tonry, J. L., Blakeslee, J. P., Dressler, A., Holtzman, J. A., Postman, M. 1997, *AJ*, 114, 626

Ajhar, E. A., Tonry, J. L., Blakeslee, J. P., Riess, A. G., & Schmidt, B. P. 2001, *ApJ*, 559, 584

Baker, J. E., Davis, M., Strauss, M. A., Lahav, O., Santiago, B. X. 1998, *ApJ*, 508, 6

Bender, R., Burstein, D., & Faber, S. M. 1993, *ApJ*, 411, 153

Blakeslee, J. P., Ajhar, E. A., & Tonry, J. L. 1999a, in *ASSL Vol. 237: Post-Hipparcos Cosmic Candles*, eds. A. Heck & F. Caputo (Boston: Kluwer), 181

Blakeslee, J. P., Davis, M., Tonry, J. L., Dressler, A., & Ajhar, E. A. 1999b, *ApJ*, 527, L73 (SBF-III)

Blakeslee, J. P., Lucey, J. R., Barris, B. J., Tonry, J. L., & Hudson, M. J. 2001a, *MNRAS*, 327, 1004 (Paper I)

Blakeslee, J. P., Vazdekis, A. & Ajhar, E. A. 2001b, *MNRAS*, 320, 193

Colless, M., Saglia, R. P., Burstein, D., Davies, R. L., McMahan R. K., & Wegner, G. 2001, *MNRAS*, 321, 277

da Costa, L. N., Nusser, A., Freudling, W., Giovanelli, R., Haynes, M. P., Salzer, J. J., & Wegner, G. 1998, *MNRAS*, 299, 425

de Vaucouleurs, G. 1961, *ApJS*, 5, 233

de Vaucouleurs, G., de Vaucouleurs, A., Corwin, H. G., Jr., Buta, R. J., Paturel, G., & Fouqué, P. 1991, *Third Reference Catalog of Bright Galaxies* (New York: Springer-Verlag) (RC3)

Djorgovski, S. & Davis, M. 1987, *ApJ*, 313, 59

Burstein, D., Faber, S. M., & Dressler, A. 1990, *ApJ*, 354, 18

Dressler, A., Lynden-Bell, D., Burstein, D., Davies, R. L., Faber, S. M., Terlevich, R. & Wegner, G. 1987, *ApJ*, 313, 42

Faber, S. M. & Jackson, R. E. 1976, *ApJ*, 204, 668

Faber, S. M., Wegner, G., Burstein, D., Davies, R. L., Dressler, A., Lynden-Bell, D. & Terlevich, R. J. 1989, *ApJS*, 69, 763

Ferrarese, L., et al. 2000, *ApJ*, 529, 745

Fisher, K. B., Huchra, J. P., Strauss, M. A., Davis, M., Yahil, A., & Schlegel, D. 1995, *ApJS*, 100, 69

Franx, M., Illingworth, G., & Heckman, T. 1989, *ApJ*, 344, 613

Freedman, W. L., et al. 2001, *ApJ*, 553, 47

Gibson, B. K. 2000, *Mem. S. A. It.*, in press (astro-ph/9910574)

Gibson, B. K. et al. 2000, *ApJ*, 529, 723

Guzmán, R., Lucey, J. R., Carter, D. & Terlevich, R. J. 1992, *MNRAS*, 257, 187

Hudson, M. J. 1994, *MNRAS*, 266, 468

Hudson, M. J. 1999, *PASP*, 111, 57

Hudson, M. J., Lucey, J. R., Smith, R. J., Schlegel, D. J., & Davies, R. L. 2001, *MNRAS*, 327, 265 (SMAC-III)

Hudson, M. J., Lucey, J. R., Smith, R. J. & Steel, J. 1997, *MNRAS*, 291, 488

Hudson, M. J., Smith, R. J., Lucey, J. R., Schlegel, D. J., & Davies, R. L. 1999, *ApJ*, 512, L79

Jensen, J. B., Tonry, J. L., Thompson, R. I., Ajhar, E. A., Lauer, T. R., Rieke, M. J., Postman, M., & Liu M. C. 2001, *ApJ*, 550, 503

Jorgensen, I., Franx, M. & Kjaergaard, P. 1993, *ApJ*, 411, 34

Jorgensen, I., Franx, M. & Kjaergaard, P. 1995, *MNRAS*, 276, 1341

Jorgensen, I., Franx, M. & Kjaergaard, P. 1996, *MNRAS*, 280, 167

Kelson, D. D. et al. 2000a, *ApJ*, 529, 768

Kelson, D. D., Illingworth, G. D., van Dokkum, P. G. & Franx, M. 2000b, *ApJ*, 531, 184

Kennicutt, Jr., R. C., et al. 1998, *ApJ*, 498, 181

Lauer, T. R., Tonry, J. L., Postman, M., Ajhar, E. A., & Holtzman, J. A. 1998, *ApJ*, 499, 577

Liu, M. C., Charlot, S. & Graham, J. R. 2000, *ApJ*, 543, 644

Lucey, J. R. & Carter, D. 1988, *MNRAS*, 235, 1177

Lucey, J. R., Currie, M. J. & Dickens, R. J. 1986, *MNRAS*, 222, 427

Lucey, J. R., Bower, R. G. & Ellis, R. S. 1991a, *MNRAS*, 249, 755

Lucey, J. R., Gray, P. M., Carter, D. & Terlevich, R. J. 1991b, *MNRAS*, 248, 804

Lucey, J. R., Guzman, R., Carter, D. & Terlevich, R. J. 1991c, *MNRAS*, 253, 584

Lynden-Bell, D., Faber, S. M., Burstein, D., Davies, R. L., Dressler, A., Terlevich, R. J., & Wegner, G. 1988, *ApJ*, 326, 19

Malmquist, K. G. 1920, *Medd. Lund. Astron. Obs., Ser. 2*, No. 22

Narayanan, V. K., Berlind, A. A., & Weinberg, D. H. 2000, *ApJ*, 528, 1

Neilsen, E. H. & Tsvetanov, Z. I. 2000, *ApJ*, 536, 255

Nusser, A. & Davis, M. 1994, *ApJ*, 421, L1

Pahre, M. A. 1998, PhD Thesis, California Institute of Technology

Pahre, M. A., Djorgovski, S. G. & de Carvalho, R. R. 1998, *AJ*, 116, 1591

Prugniel, P. & Simien, F. 1996, *A&A*, 309, 749

Riess, A. G., Davis, M., Baker, J., & Kirshner, R. P. 1997, *ApJ*, 488, L1

Sakai, S. et al. 2000, *ApJ*, 529, 698

Sandage, A. 1972, *ApJ*, 176, 21

Sandage, A. & Visvanathan, N. 1978, *ApJ*, 225, 742

Schechter, P. L. 1980, *AJ*, 85, 801

Schlegel, D. J., Finkbeiner, D. P., & Davis, M. 1998, *ApJ*, 500, 525 (SFD)

Sigad, Y., Eldar, A., Dekel, A., Strauss, M. A., & Yahil, A. 1998, *ApJ*, 495, 516

Smith, R. J., Lucey, J. R., Hudson, M. J., Schlegel, D. J., & Davies, R. L. 2000, *MNRAS*, 313, 469 (SMAC-I)

Smith, R. J., Schlegel, D. J., Lucey, J. R., Hudson, M. J., Baggley, G., & Davies, R. L. 2001, *MNRAS*, 327, 249 (SMAC-II)

Strauss, M. A. & Willick, J. A. *Phys. Rep.*, 261, 271

Tonry, J. L. 1991, *ApJ*, 373, L1

Tonry, J. L., Ajhar, E. A., & Luppino, G. A. 1990, *AJ*, 100, 1416

Tonry, J. L., Blakeslee, J. P., Ajhar, E. A., & Dressler, A. 1997, *ApJ*, 475, 399 (SBF-I)

Tonry, J. L., Blakeslee, J. P., Ajhar, E. A., & Dressler, A. 2000, *ApJ*, 530, 625 (SBF-II)

Tonry, J. L. & Davis, M. 1981, *ApJ*, 246, 680

Tonry, J. L., Dressler, A., Blakeslee, J. P., Ajhar, E. A., Fletcher, A., Luppino, G., Metzger, M. R., & Moore, C. 2001, *ApJ*, 546, 681

Tonry, J. L. & Schneider, D. P. 1988, *AJ*, 96, 807

Udalski, A., Szymanski, M., Kubik, M., Pietrzynski, G., Soszynski, I., Wozniak, P., & Zebrun, K. 1999, *Acta Astronomica*, 49, 201

van Dokkum, P. G. & Franx, M. 1996, *MNRAS*, 281, 985

Walker, A. 1999, in *ASSL Vol. 237: Post-Hipparcos Cosmic Candles*, eds. A. Heck & F. Caputo (Boston: Kluwer), 125

Willick, J. A. & Batra, P. 2001, *ApJ*, 548, 564

Willick, J. A., Strauss, M. A., Dekel, A., & Kolatt, T. 1997, *ApJ*, 486, 629

Willick, J. A. & Strauss, M. A. 1998, *ApJ*, 507, 64

Willmer, C. N. A., da Costa, L. N., & Pellegrini, P. S. 1998, *AJ*, 115, 869

**Table 1.** Summary of Distance Comparison

Comparison	Type	$v_{\max}$	$N_g$	$H_0^a$	$\chi_{\nu}^2(1p)^b$	slope <sup>c</sup>	$\chi_{\nu}^2(2p)^d$
FP vs SBF.....	all	...	164	$69.8 \pm 1.1$	1.23	$1.14 \pm 0.05$	1.20
FP vs SBF.....	E	...	111	$68.6 \pm 1.4$	0.88	$1.05 \pm 0.06$	0.91
FP vs SBF.....	all	3000	133	$68.0 \pm 1.3$	1.26	$1.15 \pm 0.06$	1.25
FP vs SBF.....	E	3000	89	$67.4 \pm 1.6$	0.89	$1.00 \pm 0.08$	0.93
FP vs SBF, red <sup>e</sup> ....	all	...	136	$70.3 \pm 1.3$	1.18	$1.11 \pm 0.05$	1.17
FP vs SBF, red <sup>e</sup> ....	E	...	94	$68.4 \pm 1.5$	0.80	$1.05 \pm 0.06$	0.84
FP vs SBF, red <sup>e</sup> ....	all	3000	105	$68.2 \pm 1.5$	1.20	$1.10 \pm 0.07$	1.20
FP vs SBF, red <sup>e</sup> ....	E	3000	72	$66.9 \pm 1.8$	0.79	$0.98 \pm 0.09$	0.83
SBF vs <i>IRAS</i> .....	all	...	164	$75.4 \pm 0.9$	1.08	$1.00 \pm 0.03$	1.09
SBF vs <i>IRAS</i> .....	E	...	111	$75.3 \pm 1.1$	1.18	$1.02 \pm 0.04$	1.20
SBF vs <i>IRAS</i> .....	all	3000	133	$74.1 \pm 1.1$	1.00	$1.13 \pm 0.05$	0.96
SBF vs <i>IRAS</i> .....	E	3000	89	$74.2 \pm 1.2$	1.13	$1.20 \pm 0.07$	1.04
FP vs <i>IRAS</i> .....	all	...	164	...	1.18	$1.10 \pm 0.05$	1.16
FP vs <i>IRAS</i> .....	E	...	111	...	1.08	$1.07 \pm 0.06$	1.07
FP vs <i>IRAS</i> .....	all	3000	133	...	1.23	$1.32 \pm 0.08$	1.09
FP vs <i>IRAS</i> .....	E	3000	89	...	1.13	$1.30 \pm 0.11$	1.05
FP vs <i>IRAS</i> , red <sup>e</sup> ...	all	...	136	...	1.11	$1.09 \pm 0.05$	1.09
FP vs <i>IRAS</i> , red <sup>e</sup> ...	E	...	94	...	0.93	$1.07 \pm 0.06$	0.93
FP vs <i>IRAS</i> , red <sup>e</sup> ...	all	3000	105	...	1.15	$1.32 \pm 0.09$	1.02
FP vs <i>IRAS</i> , red <sup>e</sup> ...	E	3000	72	...	0.97	$1.29 \pm 0.12$	0.89
$\overline{N}$ SBF vs <i>IRAS</i> <sup>f</sup> ...	all	...	164	$76.2 \pm 0.9$	0.96	$0.97 \pm 0.03$	0.96
$\overline{N}$ SBF vs <i>IRAS</i> <sup>f</sup> ...	E	...	111	$76.4 \pm 1.1$	1.07	$0.98 \pm 0.04$	1.08
$\overline{N}$ SBF vs <i>IRAS</i> <sup>f</sup> ...	all	3000	133	$74.8 \pm 1.0$	0.87	$1.09 \pm 0.05$	0.86
$\overline{N}$ SBF vs <i>IRAS</i> <sup>f</sup> ...	E	3000	89	$74.9 \pm 1.2$	1.01	$1.15 \pm 0.07$	0.96

<sup>a</sup> These values of  $H_0$  are derived from the SBF-II direct calibration, based on the Cepheid distances tabulated by Ferrarese et al. (2000); changing to the revised Cepheid distances of Freedman et al. (2001) would increase each  $H_0$  by 2.8% (see Ajhar et al. 2001).

<sup>b</sup> Reduced  $\chi^2$  for a single parameter ( $H_0$ ) fit between the two sets of distances.

<sup>c</sup> Best-fitting slope for a 2-parameter, bivariate linear fit of the first set of distances as a function of the second set.

<sup>d</sup> Reduced  $\chi^2$  for the 2-parameter fit.

<sup>e</sup> ‘Red’ subsample defined in Paper I: galaxies with  $(V-I)_0 \geq 1.135$ .

<sup>f</sup> Adopts the  $\overline{N}$ -distance calibration of Eq. (4); the fact that the resulting  $H_0$ ’s are all 1% larger than those from the standard SBF method implies a  $\sim 0.02$  mag offset of the SBF-IV  $\overline{N}$  calibration with respect to the SBF-II  $(V-I)_0$  calibration.